USGS
science for a changing world

Prepared in cooperation with the Bureau of Reclamation

Hydrogeologic and Geochemical Characterization and Evaluation of Two Arroyos for Managed Aquifer Recharge by Surface Infiltration in the Pojoaque River Basin, Santa Fe County, New Mexico, 2014–15

Scientific Investigations Report 2017–5007

U.S. Department of the Interior
U.S. Geological Survey

Cover:

Top, Photograph of study area landscape and Tesuque Formation outcrops by Andrew Robertson, U.S. Geological Survey.

Left, Photograph of U.S. Geological Survey (USGS) personnel preparing to sample the Windmill Well by Andrew Robertson, USGS.

Right, Photograph of U.S. Geological Survey (USGS) Auger rig set to start drilling in ASR-East at site BH-4 by Andrew Robertson, USGS.

Hydrogeologic and Geochemical Characterization and Evaluation of Two Arroyos for Managed Aquifer Recharge by Surface Infiltration in the Pojoaque River Basin, Santa Fe County, New Mexico, 2014–15

By Andrew J. Robertson, Jeffery Cordova, Andrew Teeple, Jason Payne, and Rob Carruth

Prepared in cooperation with the Bureau of Reclamation

Scientific Investigations Report 2017–5007

U.S. Department of the Interior
U.S. Geological Survey

U.S. Geological Survey
William H. Werkheiser, Acting Director

U.S. Geological Survey, Reston, Virginia: 2017

For more information on the USGS—the Federal source for science about the Earth, its natural and living resources, natural hazards, and the environment—visit http://www.usgs.gov or call 1–888–ASK–USGS.

For an overview of USGS information products, including maps, imagery, and publications, visit http://store.usgs.gov.

Suggested citation:
Robertson, A.J., Cordova, Jeffery, Teeple, Andrew, Payne, Jason, and Carruth, Rob, 2017, Hydrogeologic and geochemical characterization and evaluation of two arroyos for managed aquifer recharge by surface infiltration in the Pojoaque River Basin, Santa Fe County, New Mexico, 2014–15: U.S. Geological Survey Scientific Investigations Report 2017–5007, 37 p., https://doi.org/10.3133/sir20175007.

ISSN 2328-0328 (online)

Acknowledgments

The authors would like to acknowledge the people of the Pueblo of Pojoaque for their support and insight during this investigation.

Contents

Figures

Tables

Conversion Factors

U.S. customary units to International System of Units

Multiply	By	To obtain
	Length	
inch (in.)	2.54	centimeter (cm)
foot (ft)	0.3048	meter (m)
mile (mi)	1.609	kilometer (km)
	Volume	
gallon (gal)	3.785	liter (L)
gallon (gal)	0.003785	cubic meter (m^3)
acre-foot (acre-ft)	1,233	cubic meter (m^3)
	Flow rate	
cubic foot per second (ft^3/s)	0.02832	cubic meter per second (m^3/s)
gallon per minute (gal/min)	0.06309	liter per second (L/s)
	Hydraulic conductivity	
foot per day (ft/d)	0.3048	meter per day (m/d)

Temperature in degrees Celsius (°C) may be converted to degrees Fahrenheit (°F) as follows:

$$°F = (1.8 \times °C) + 32.$$

Temperature in degrees Fahrenheit (°F) may be converted to degrees Celsius (°C) as follows:

$$°C = (°F - 32) / 1.8.$$

Datum

Vertical coordinate information is referenced to the North American Vertical Datum of 1988 (NAVD 88).

Horizontal coordinate information is referenced to the North American Datum of 1983 (NAD 83).

Altitude, as used in this report, refers to distance above the vertical datum.

Supplemental Information

Specific conductance is given in microsiemens per centimeter at 25 degrees Celsius (µS/cm at 25 °C).

Concentrations of chemical constituents in water are given in either milligrams per liter (mg/L) or micrograms per liter (µg/L).

Abbreviations

<	less than
$\delta^{18}O$	delta oxygen-18
δD	delta deuterium
2-D	two-dimensional
3-D	three-dimensional
^{3}H	tritium
^{12}C	carbon-12
^{13}C	carbon-13
^{14}C	carbon-14
ASR	aquifer storage and recovery
ASTM	American Society for Testing and Materials
BH	borehole
Ca	calcium
CMB	chloride mass balance
CO_2	carbon dioxide
Cu	copper
DC	direct current
DIC	dissolved inorganic carbon
DS	dissolved solids
EPA	U.S. Environmental Protection Agency
ET	evapotranspiration
FDEM	frequency-domain electromagnetics
Fe	iron
GMWL	Global Meteoric Water Line
GPS	Global Positioning System
HCO_3	bicarbonate
HEC-RAS	Hydrologic Engineering Center's Rivers Analysis System
MCL	maximum contaminant level
MW	Monitoring Well
Na	sodium
NO_3	nitrate
NWIS	National Water Information System
OPUS	Online Positioning User System
PBRWS	Pojoaque Basin Regional Water System
PVC	polyvinyl chloride
ppm	parts per million
Reclamation	Bureau of Reclamation
RPD	relative percent difference
RTK	Real-Time Kinematic
Rx	receiver
SAC-GUI	Slope-Area Computation Graphical User Interface
SC	specific conductance
SO_4	sulfate
USGS	U.S. Geological Survey
TU	tritium units
Tx	transmitter
VSMOW	Vienna Standard Mean Ocean Water
XRD	X-ray diffraction

Hydrogeologic and Geochemical Characterization and Evaluation of Two Arroyos for Managed Aquifer Recharge by Surface Infiltration in the Pojoaque River Basin, Santa Fe County, New Mexico, 2014–15

By Andrew J. Robertson, Jeffery Cordova, Andrew Teeple, Jason Payne, and Rob Carruth

Abstract

In order to provide long-term storage of diverted surface water from the Rio Grande as part of the Aamodt water rights settlement, managed aquifer recharge by surface infiltration in Pojoaque River Basin arroyos was proposed as an option. The initial hydrogeologic and geochemical characterization of two arroyos located within the Pojoaque River Basin was performed in 2014 and 2015 in cooperation with the Bureau of Reclamation to evaluate the potential suitability of these two arroyos as sites for managed aquifer recharge through surface infiltration.

The selected reaches were high-gradient (average 3.0–3.5 percent) braided channels filled with unconsolidated sand and gravel-sized deposits that were generally 30–50 feet thick. Saturation was not observed in the unconsolidated channel sands in four subsurface borings but was found at 7–60 feet below the contact between the unconsolidated channel sands and the bedrock. The poorly to well-cemented alluvial deposits that make up the bedrock underlying the unconsolidated channel material is the Tesuque Formation. The individual beds of the Tesuque Formation are reported to be highly heterogeneous and anisotropic, and the bedrock at the site was observed to have variable moisture and large changes in lithology. Surface electrical-resistivity geophysical survey methods showed a sharp contrast between the electrically resistive unconsolidated channel sands and the highly conductive bedrock; however, because of the high conductivity, the resistivity methods were not able to image the water table or preferential flow paths (if they existed) in the bedrock.

Infiltration rates measured by double-ring and bulk infiltration tests on a variety of channel morphologies in the study reaches were extremely large (9.7–94.5 feet per day), indicating that the channels could potentially accommodate as much as 6.6 cubic feet per second of applied water without generating surface runoff out of the reach; however, the small volume available for storage in the unconsolidated channel sands (about 410 acre-feet in the east arroyo and about 190 acre-feet in the west arroyo) and the potential for the infiltrating water to preferentially flow over the bedrock contact and out of the reach present a challenge for storing water. Although a detailed assessment of the infiltration rate of the Tesuque Formation is beyond the scope of this investigation, one double-ring infiltrometer test was conducted on an outcrop, resulting in an estimated infiltration rate of about 4 feet per day.

The shallow groundwater observed in this investigation was determined to be recharged locally on the basis of groundwater elevations and geochemical and isotopic signatures. The channel sands and shallow bedrock were observed to be weathered, indicating contact with oxic groundwater following deposition. This observation was supported by whole-rock elemental analysis and mineralogy of several core samples. The downward groundwater gradient between the shallow wells and those wells screened at greater depths suggests that the shallow groundwater is recharged by local precipitation and has the potential to migrate to the deeper aquifer units. The two age-dating tracers measured in this investigation, however, demonstrate that the shallow groundwater flow paths are very slow and that the deeper flow paths are likely part of a larger regional system.

The composition of the shallow, native groundwater suggests that storing water diverted from the Rio Grande is not likely to leach constituents of concern that would cause the stored water to exceed health-based U.S. Environmental Protection Agency Maximum Contaminant Levels.

Introduction

Water rights in the Pojoaque River Basin in northern New Mexico were the subject of the long-running adjudication known as the Aamodt case (*State of New Mexico* v. *Aamodt et al.* [U.S. District Court No. 6639 (D.N.M.)]). The adjudication process is a legal method to determine the priority and amount of water rights for users in a basin. The adjudication of the Nambé-Pojoaque-Tesuque stream systems began in 1966,

and the parties included the Pueblos of Nambé, Pojoaque, San Ildefonso, and Tesuque; various Federal, State, and local agencies; and a number of non-Indian claimants (Chestnut, 2012). The Aamodt case was initiated, in part, to distribute and account for water imported to the Pojoaque River Basin through the San Juan-Chama Project, a project that transfers a portion of water from the Colorado River to the Rio Grande (Chestnut, 2012). Forty years later, in February 2006, the claimants agreed upon and signed a settlement. Congress passed the Claims Resolution Act in 2010 approving the Aamodt case and other settlements.

The Claims Resolution Act (P.L. 111-291, Title VI) authorized the Secretary of the Interior, acting through the Commissioner of the Bureau of Reclamation (Reclamation), to plan, design, and construct the Pojoaque Basin Regional Water System (PBRWS) in the Pojoaque River Basin in Santa Fe County, N. Mex (fig. 1). The PBRWS is intended to provide reliable potable water, reduce reliance on groundwater, and allow the pueblos to obtain additional water rights (HKM Engineering, 2008). One component of the PBRWS was the construction of aquifer storage and recovery (ASR) wells to provide long-term storage of diverted surface water in the local aquifers. An evaluation of the feasibility of the PBRWS by HKM Engineering (2008) described the need for three 400-gallons-per-minute (gal/min) wells, which would provide approximately half of the average daily water-use requirements of the Pojoaque River Basin.

In 2013, the U.S. Geological Survey (USGS), in cooperation with Reclamation, installed an exploratory observation well to characterize the local hydrologic conditions and evaluate the potential of the proposed site for installing wells to implement the ASR component of the PBRWS (S.E. Falk, D. O'Leary, C.R. Harich, J.R. Masoner, and J.V. Thomas, U.S. Geological Survey, written commun., 2014). The observation well was screened at various intervals between 640 and 1,500 feet (ft) below land surface (bls) in the Santa Fe Group aquifer. The investigation concluded that the upward vertical hydraulic gradient observed at the site would have required forced injection of recharge water and that the confined conditions indicated low storativity. In addition, the geochemical conditions in the aquifer represented contrasting characteristics to Rio Grande water that may have caused precipitation and (or) mobilization of chemical constituents. It was therefore determined that the site presented technical challenges and would not be optimal for the implementation of that project component. In response, managed aquifer recharge by surface infiltration in Pojoaque River Basin arroyos was proposed as an alternative. Managed aquifer recharge has been used to augment natural recharge, to replenish aquifers depleted by pumping, and to store water during wetter years for withdrawal during drier years (Dillon, 2005; National Research Council, 2008). The USGS, in cooperation with Reclamation, conducted an initial hydrogeologic and geochemical characterization of two arroyos located in the Pojoaque River Basin to evaluate the potential for managed aquifer recharge through surface infiltration.

Purpose and Scope

This report describes the collection and evaluation of hydrogeologic and geochemical data collected during 2014 and 2015 from two ephemeral arroyos located within the Pojoaque River Basin. The data are used to provide an initial hydrogeologic and geochemical characterization of two arroyos to assess the potential of using managed aquifer recharge through surface infiltration as a method of storing diverted Rio Grande surface water.

Description of Study Area

The study area is located in northern Santa Fe County, about 2 miles (mi) southwest of the town of Pojoaque in north-central New Mexico (fig. 1). The two ephemeral arroyos that are the focus of the study are located south of New Mexico State Road 502 and just east of the Pojoaque Valley High School (fig. 2). The arroyos, Arroyo de Jaconito (hereinafter referred to as "ASR-West") and an unnamed arroyo (hereinafter referred to as "ASR-East"), drain to the Pojoaque River and are part of the Pojoaque River Basin in northern Santa Fe County. Within each of the arroyos, a reach of approximately 2,500 linear ft was selected for the study.

The study reaches are high-gradient braided channels with sand- and gravel-sized bed material. The channel bottoms are devoid of vegetation, but small shrubs, grasses, and piñon trees are interspersed on bars between the channels and crowd the banks of the channels. The two arroyos drain runoff from outcrops of the Tesuque Formation, a member of the alluvial Santa Fe Group. Access to the two reaches is limited, and the primary route to the reaches is in the channel itself.

Geology

The site is located in the Española structural basin (hereinafter referred to as "Española Basin") (fig. 1), an alluvial-fill basin formed by the east-west crustal extension of the Cenozoic Rio Grande rift. The Española Basin is bound to the west by the Jemez Mountains and to the east by the Sangre de Cristo Mountains (Dethier and Reneau, 1995). The primary structure in the Española Basin is a west-tilted graben that formed during the east-west extensional rifting. Faulting in the Española Basin tends to be normal, and faults are oriented north-northeast (Kelley, 1978). The Española Basin is filled with eolian, fluvial, and alluvial sediments of the Santa Fe Group that are interbedded with volcanic deposits and volcanoclastic sediments. The base of the sedimentary layers is tilted as much as 17 degrees to the west (Koning and Read, 2010).

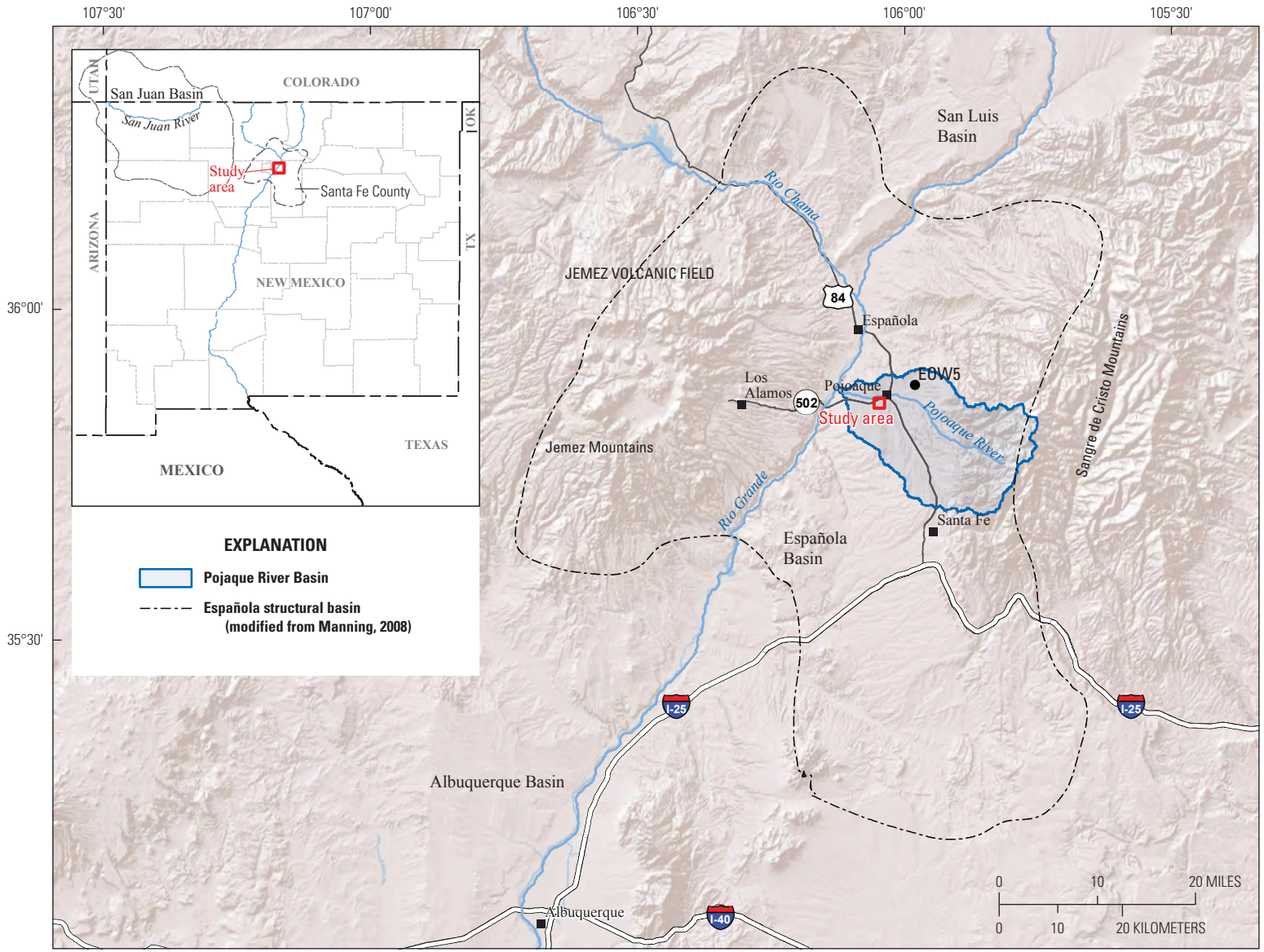

Figure 1. The location of study area, Pojoaque, New Mexico.

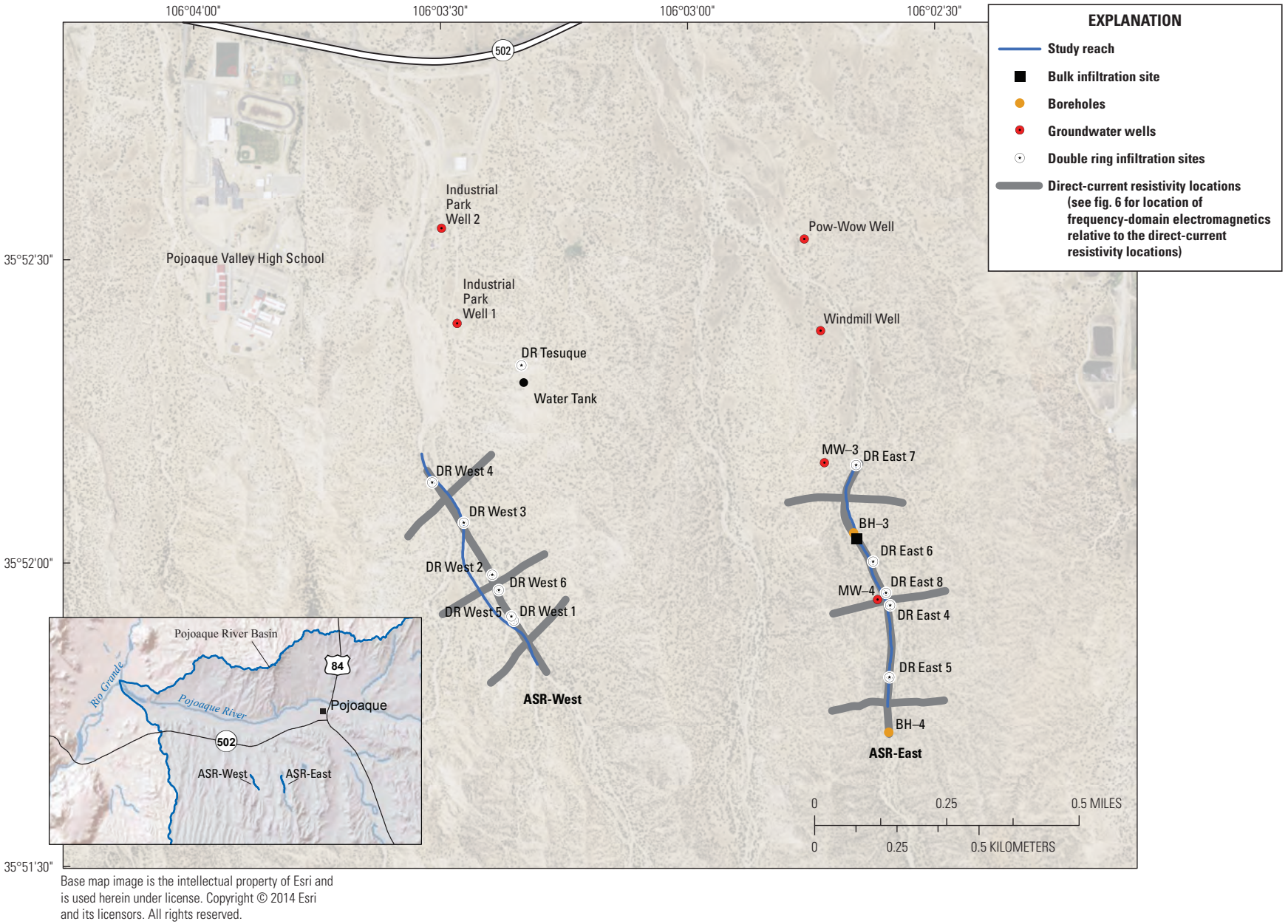

Figure 2. Location of groundwater wells, boreholes, direct-current resistivity locations, and infiltration sites, Pojoaque River Basin, New Mexico.

The basin-fill silts, sands, and clays of the Santa Fe Group are predominantly derived from the Precambrian igneous and metamorphic rocks and the overlying Paleozoic sedimentary rocks of the Sangre de Cristo Mountains to the east and the Tertiary volcanic rocks of the Jemez Mountains to the west (fig. 1). The thickness of the Santa Fe Group varies over the Española Basin, with a maximum thickness of more than 10,000 ft. In the general area of the study, the Santa Fe Group is approximately 7,500 ft thick near the Rio Grande and thins eastward to approximately 3,500 ft thick at the study area (Koning and Read, 2010).

The Santa Fe Group is divided into three formations: the Tesuque Formation, the Chamita Formation, and the Puye Formation. The Miocene Tesuque Formation is the principal aquifer-forming unit of the Santa Fe Group in the study area (Manning, 2008) and is the most widely exposed (Galusha and Blick, 1971), and, therefore, is described here in detail. It is composed of poorly to well-cemented silt, sand, clay, gravel, and cobbles. The sediments are predominantly composed of fragments of Precambrian-age quartz, feldspar, granite, schist, gneiss, and quartzite rocks with cementation by calcium carbonate. Clay is present throughout the formation, and silts and very fine grained sands compose the largest part of the formation (Spiegel and Baldwin, 1963). The Tesuque Formation was deposited predominantly as alluvial fans; however, basalt flows and interbedded tuff layers are present locally. These volcanic deposits are thought to be the source of uranium (U), arsenic (As), and fluoride (F) that are present in water from many wells in the Pojoaque River Basin at concentrations that exceed the U.S. Environmental Protection Agency (EPA) Maximum Contaminant Levels (MCLs) (McQuillan and Montes, 1998; McLemore and others, 2011). Beds in the Tesuque Formation dip between 5 and 10 degrees, and local fault blocks may dip as much as 30 degrees (Kelley, 1979; Hearne, 1985), having been displaced by several north-south trending normal faults (McQuillan and Montes, 1998).

Climate

The present climate is semiarid to arid in the lower elevations of the Española Basin and semiarid above 5,900 ft (Dethier and Reneau, 1995). The average annual precipitation (1895–2012) in Española, N. Mex., about 8.5 mi north of the site, is 9.88 inches (in.), with almost half of the annual precipitation falling in the monsoon season of July through September (Western Regional Climate Center, 2016).

Surface-Water Hydrology

The arroyos in the study area are dry and flow only in response to precipitation runoff. These arroyos drain to the ephemeral Pojoaque River, which is a tributary of the Rio Grande (fig. 2). The Rio Chama flows into the Rio Grande approximately 11.3 mi above the confluence of the Rio Grande and Pojoaque River (fig. 1). There is no discharge record for the Pojoaque River, but the river was observed to be mostly dry during the investigation.

Groundwater Hydrology

The principal aquifer-forming unit of the Santa Fe Group in the area of the Pojoaque River Basin is the Tesuque Formation (Manning, 2008). Groundwater flow in the study area, based on water-level contour maps, is to the west-northwest from mountain-front recharge in the Sangre de Cristo Mountains to the Rio Grande (McAda and Wasiolek, 1988; Anderholm, 1994; Manning, 2008). Groundwater elevations in the study area generally range from around 5,500 ft near the Rio Grande to 7,600 ft in the Sangre de Cristo Mountains. Vertical gradients are downward along the mountain front and upward in most areas west of the mountain front (Johnson and others, 2013). The vertical gradients and artesian conditions documented in well Exploratory Observation Well 5 (EOW5), installed for the 2013 ASR investigation, indicated that confining conditions exist near the study area (S.E. Falk, D. O'Leary, C.R. Harich, J.R. Masoner, and J.V. Thomas, U.S. Geological Survey, written commun., 2014).

These groundwater descriptions represent the larger Española Basin and may not adequately represent local hydraulic gradients and water levels. The Tesuque Formation has been characterized by Hearne (1985) as dipping, heterogeneous, anisotropic, limited areally, and disrupted by faulting, making extrapolation of aquifer properties between areas difficult.

Previous Investigations

Hearne (1985) developed a three-dimensional digital model of the groundwater-flow system of the Pojoaque River Basin to simulate the response of the aquifer system to withdrawals for irrigation. The Tesuque Formation was represented as continuous layers aligned along the small regional dip to the west-northwest (Hearne, 1985). Simulated withdrawals of groundwater (15,280 gal/min [24,650 acre-feet (acre-ft) per year] for 50 years) for an irrigation-development plan resulted in reductions in aquifer storage, declines in water levels of up to 334 ft, and capture of streamflow from the Rio Grande and Pojoaque River (Hearne, 1985). Hearne (1985) reported that the hydraulic-head computations for the model were most sensitive to variations in hydraulic conductivity.

A study of the feasibility of the proposed PBRWS, the Aamodt Feasibility Study, was completed in 2002 as a collaborative report by Reclamation and consultants to provide additional technical details and estimated capital and operating costs for the system. The final report for task 3 of the study covered the feasibility of proposed deep ASR wells for supplemental supply, injection wells for storage of surface water in the aquifer, and integration of the wells into the regional system (Arctic Slope Consulting Group

and John Shomaker and Associates, Inc., 2003). The report summarized the regional geology and hydrogeology, selected water-quality data, selected well-property data, and other data to make recommendations for production well-field locations, proposed well design and yield estimates, and cost estimates (Arctic Slope Consulting Group and John Shomaker and Associates, Inc., 2003). The final report indicated that the target zone for well installation should be the Nambé Member of the Tesuque Formation, which was reported to contain water of good quality, with concentrations of U, As, and total dissolved solids generally less than the MCLs (Arctic Slope Consulting Group and John Shomaker and Associates, Inc., 2003). A later investigation revised the evaluations of the original ASR well locations described in the 2003 report on the basis of updated geologic maps of the area (HKM Engineering, 2008). That investigation included detailed descriptions of local geologic conditions and estimated depths of selected geologic units and made recommendations for aquifers that might be used for ASR.

Study Methods

The characterization and evaluation of two ephemeral arroyos near the town of Pojoaque, N. Mex., for use as a managed aquifer recharge site through surface infiltration was completed by the collection and analysis of hydrogeologic and geochemical data. Data were collected by the USGS in November and December 2014 and January 2015 (fig. 2, table 1).

Hydrogeologic Characterization Methods

The methods used to characterize the hydrogeology of the site included a survey of the channel geometries and adjacent terraces, a geophysical investigation, continuous core borings, surface-infiltration tests, and groundwater levels. A description of these methods is described below.

Survey of the Arroyos and Adjacent Terrace and Water-Surface Profile Calculations

In order to determine the conveyance capacity of the stream channel and establish baseline channel conditions, survey-grade positions were measured with Global Positioning System (GPS) equipment, and slope-area calculations (Dalrymple and Benson, 1967) were performed to model bankfull conditions. Spatial locations and elevations for this project were determined by using the Real-Time Kinematic (RTK) survey technique with Topcon survey-grade equipment. A reference point for the RTK network was established by occupying and collecting GPS data and referencing it to the National Spatial Reference System (NAD83[2011] epoch 2010.00) by using the Online Positioning User System (OPUS) (National Geodetic Survey, 2015). A pre-established rebar survey marker, located on top of a hill approximately 50 ft south of the water tank (fig. 2), was used as the base for this survey. The OPUS occupation was a rapid-static survey that collected GPS data for 1 hour and 19 minutes. Nine National Geodetic Survey Continuously Operating Reference Stations were used in OPUS processing, and 94 percent of the observations were used to produce an overall normalized root mean square error of 0.258.

The RTK survey was performed on ASR-East and ASR-West within the study area to determine their cross-section geometry and channel slope. A total of 640 discrete points were measured. The points were collected every 5–10 ft along transects perpendicular to each arroyo or where there was an obvious change in the channel slope. Points were also collected approximately every 50 ft along the channel to determine slope. The locations and elevations of the Pow-Wow Well (site number 355233106024501), the Windmill Well (site number 355224106024301), Monitoring Well–3 (MW–3; site number 355208106024201), and MW–4 (site number 355152106023801) were also determined by RTK. The elevations of the wells were determined so that groundwater levels could be referenced to a common datum. MW–3 and MW–4 were surveyed at a brass survey marker installed in the well pad; the Pow-Wow and Windmill Wells were surveyed at a point on the casing. Borehole–3 (BH–3) and BH–4 were surveyed following drilling at the land surface where the borings occurred.

The RTK survey data of the ASR-West and ASR-East channel dimensions were postprocessed with the Slope-Area Computation Graphical User Interface (SAC-GUI) (Bradley, 2012). The SAC-GUI program was used to calculate the distance between each surveyed point. The channel dimensions were imported into the Hydrologic Engineering Center's Rivers Analysis System (HEC-RAS) version 4.1 to compute water-surface profiles for several discharges to determine flow characteristics for the channels (U.S. Army Corps of Engineers, 2010).

Subsurface Characterization

To evaluate storage capacity of the underlying deposits and potential barriers or preferential pathways for infiltrating flows, subsurface electrical resistivity was measured with surface geophysics, and four boreholes were completed into the bedrock. Continuous cores were collected from the land surface to the depth of saturation. Samples from those cores were analyzed for elemental chemistry and mineralogy.

Surface Geophysics

Surface geophysical resistivity methods can be used to detect spatial changes in the electrical properties of the subsurface by using noninvasive surface-based instrumentation (Zohdy and others, 1974). The electrical properties of soils and rocks are affected by water content,

Table 1. Site information and type of data collected for surface infiltration study, Pojoaque, New Mexico.

[The epoch date indicates that the published coordinates represent the location of the control stations on January 1, 2010 (National Geodetic Survey, 2015). Geoid12A is the August 10, 2012, model for transforming heights between ellipsoidal coordinates and physical height systems that relate to water flow. USGS, U.S. Geological Survey; NAD 83, North American Datum of 1983; NAVD 88, North American Vertical Datum of 1988; DR, double ring; MW, monitoring well; BH, borehole]

Site name	USGS site identifier	Latitude	Longitude	Elevation	Type of data
		NAD 83 (2011) (epoch: 2010.00)		feet NAVD 88 (Geoid12A)	
Survey benchmarks					
Water tower		35.872141	-106.055073	5,933.3	Vertical and horizontal controls
Double ring infiltration measurements					
DR East-4	355158106023501	35.866087	-106.043062	6,002.3	Infiltration rate
DR East-5	355150106023501	35.863772	-106.042921	6,031.8	Infiltration rate
DR East-6	355201106023701	35.866949	-106.043505	5,991.5	Infiltration rate
DR East-7	355211106023901	35.869594	-106.044116	5,955.7	Infiltration rate
DR East-8	355157106023501	35.865746	-106.042924	6,007.2	Infiltration rate
DR West-1	355155106032001	35.865221	-106.055611	5,931.1	Infiltration rate
DR West-2	355159106032301	35.866467	-106.056347	5,913.1	Infiltration rate
DR West-3	355201106032601	35.867892	-106.057330	5,894.0	Infiltration rate
DR West-4	355208106033001	35.868991	-106.058419	5,881.6	Infiltration rate
DR West-5	355155106032101	35.865328	-106.055690	5,930.1	Infiltration rate
DR West-6	355158106032201	35.866054	-106.056120	5,920.3	Infiltration rate
DR-Tesuque	355220106032001	35.872236	-106.055438	5,921.9	Infiltration rate
Bulk infiltration test					
Bulk infiltration site	355203106023801	35.867563	-106.044078	5,981.6	Infiltration rate
Groundwater wells					
Industrial Park Well 1	355224106032801	35.873363	-106.057629	5,869.4	Water levels and water quality
Industrial Park Well 2	355233106032901	35.875980	-106.058192	5,836.6	Water levels
Pow-Wow Well	355233106024501	35.875787	-106.045948	5,881.78	Water levels and water quality
Windmill Well	355224106024301	35.873275	-106.045361	5,908.13	Water levels and water quality
MW-3	355208106024201	35.869652	-106.045182	5,961.51	Water levels and water quality
MW-4	355152106023801	35.865906	-106.043346	6,009.13	Water levels and water quality
Boreholes					
BH-3	355207106024001	35.867728	-106.044180	5,979.3	Water levels
BH-4	355147106023501	35.862266	-106.042923	6,049.0	Water levels

grain size, porosity, clay content, and the conductivity (reciprocal of electrical resistivity) of the pore water (Lucius and others, 2007). Interpretation of the spatial distribution of subsurface electrical properties from resistivity measurements can then be used to describe differences in the subsurface hydrogeology.

The two surface geophysical resistivity methods used to evaluate the hydrogeology in the two arroyos were two-dimensional (2-D) direct-current (DC) resistivity and frequency-domain electromagnetics (FDEM). Generally, the 2-D DC resistivity method allows for deeper resistivity measurements, whereas the FDEM method allows for greater spatial data density. The dual-method approach was used to achieve a more comprehensive analysis of the subsurface and to accurately estimate the thickness, extent, and lateral variation in the resistivity of the subsurface. About 14,800 ft of 2-D DC resistivity survey profiles (fig. 2) and about 8 mi of continuous FDEM survey lines were collected at the site.

Direct-Current Resistivity Profiles

The IRIS Instruments Syscal Pro system (IRIS Instruments, 2015) was used to collect eight 2-D DC profiles of apparent resistivity. Each arroyo had one longitudinal line

traversing the selected length of the arroyo reach and three lines approximately perpendicular to the arroyo (fig. 2). The longitudinal lines were collected with an electrode spacing of 3 meters (m), whereas the perpendicular lines were collected with an electrode spacing of 5 m. The 2-D DC resistivity methods used in this study use an array of four electrodes (two transmitter [Tx] electrodes and two receiver [Rx] electrodes) inserted in the soil to measure bulk electrical resistivity in the subsurface. DC data were collected by using both a dipole-dipole and reciprocal Schlumberger array. More discussion on DC surveying and array configurations can be found in Burton and others (2014). Visual inspection of apparent resistivity pseudosections for each of the arrays and reciprocals was used to verify that no equipment- or field-induced biases occurred during data collection. The raw field data (current and voltage) also were reviewed for measurement uncertainty by using Prosys II version 2.15 (IRIS Instruments, 2015) to evaluate the minimum and maximum current and voltage and the standard deviation of the computed apparent-resistivity data. A few data points were removed from each profile by using the "estimate bad data points" option in the Prosys II software.

The sinuous nature of the arroyo led to the need for a three-dimensional (3-D) inversion algorithm; therefore, the apparent 2-D DC resistivity data were inverted by using ERTLab release 1.0 (Multiphase Technologies, 2015). Because of both computer hardware and software limitations, each profile had to be divided into multiple smaller segments before being inverted. The segments were later stitched back together to create one continuous profile by using the ERT Lab software. No loss of spatial or computational integrity occurred during the segmentation and restitching process.

Frequency-Domain Electromagnetic Survey

The FDEM method complements the 2-D DC resistivity method and can be useful for quality assurance and control by visually comparing resistivity profiles obtained by using each method. The FDEM method uses multiple current frequencies to measure bulk conductivity values (the inverse of resistivity values) of the earth at different depths (Lucius and others, 2007).

FDEM data were collected with a GEM-2, a broadband multifrequency fixed-coil electromagnetic induction unit (Geophex, 2015), near the same transects as the 2-D DC resistivity data. The unit has a fixed spacing (1.67 m) between the Tx and Rx coils, with a bucking coil between them to remove the primary magnetic field from the Rx signal. The unit records the in-phase and quadrature responses (in units of parts per million) of the primary field, which represent the scaled ratio of the secondary magnetic field to the primary magnetic field at the receiver coil. More information about the GEM-2 and its operating principles are discussed in Won and others (2006).

The GEM-2 was operated in vertical-dipole mode (horizontal coplanar coils or loops) at 15 frequencies. Although no power-transmission lines were present in the immediate area, the 60-hertz (Hz) frequency was monitored throughout the survey to avoid harmonic frequencies of 60 Hz.

Over the course of collecting measurements with the GEM-2 unit, the instrument had the potential for drift because of conditions such as battery voltage depletion or temperature variations. To allow for drift correction, leveling stations were established to compare static measurements (no operator movement) over time to a single reference measurement. Multiple times throughout the survey, the GEM-2 was placed at these leveling stations, and approximately 3–5 minutes of data were collected for drift correction.

Drilling and Well Construction Methods

The USGS Research Drilling Group used an auger rig to drill two boreholes (BH–3 and BH–4), which were plugged after collecting a static water-level and two other borings that were completed as groundwater monitoring wells (MW–3 and MW–4) in ASR-East (fig. 2, table 1). The hollow-stem auger method was used to collect continuous core samples from the borings with a 4.25-in. split-barrel sampling tube (fig. 3). The 8-in.-diameter auger was advanced at alternating 2- or 3-ft intervals to the termination of the borehole. In between borings, the augers and drill stem were cleaned by using a high-pressure sprayer.

BH–3 and BH–4 were drilled in the arroyo bottom to characterize the underlying lithology. BH–3 was drilled to a depth of 61.5 ft bls, and BH–4 was drilled to a depth of 69.5 ft bls. After collecting a static water level, BH–3 and BH–4 were abandoned in place by using grout and bentonite chips to backfill the borehole.

The monitoring wells (MW–3 and MW–4) were installed on the terrace adjacent to ASR-East at the upstream and downstream end of the reach (fig. 2, table 1). MW–3 and MW–4 were completed below the water table at depths of 124 ft and 87 ft, respectively. Wells were constructed by using 2-in. schedule-40 polyvinyl chloride (PVC) risers, with 20 ft of 0.10-slotted PVC screen in MW–3 and 35 ft of 0.10-slotted PVC screen in MW–4. Each well was installed with a 5-ft section of blank casing below the screen. A 4- by 4-ft concrete pad and an 8-in. steel riser well-vault with a locking cap was installed at the surface to protect the wells (fig. 3).

Surface Infiltration Tests

To determine the rate at which water applied to the stream channel will infiltrate into the channel deposits, surface infiltration tests were performed at various locations in the stream channel. Infiltration is the downward entry of surface water into the underlying soil or sediment (Johnson, 1963). The infiltration rate is the volume of water per unit area entering the subsurface per unit of time. The rate generally decreases as the sediments become saturated. The factors in the subsurface that influence the infiltration rate include the sediment structure, the condition of the surface, the amount and distribution of soil moisture, and the chemical

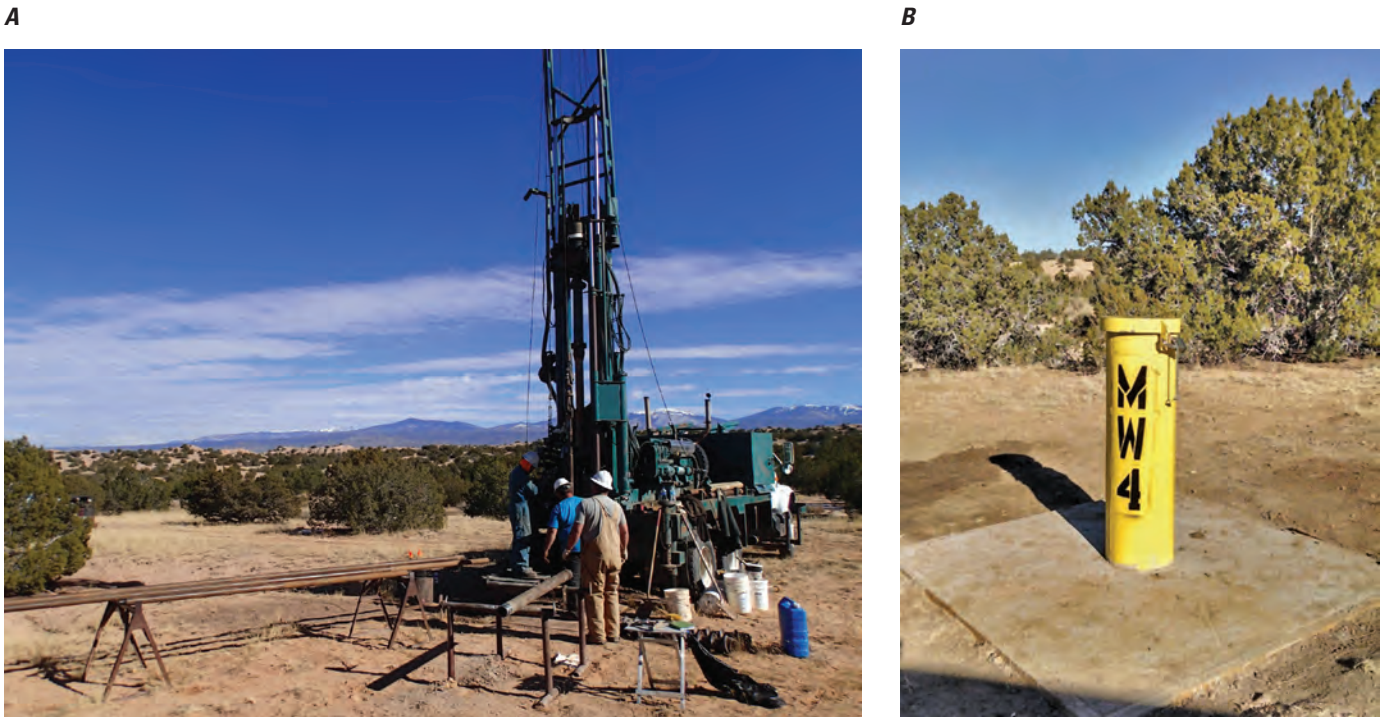

Figure 3. An auger drill rig (*A*) and completed monitoring well (*B*), Pojoaque, New Mexico.

and physical natures of the sediments (Johnson, 1963). Characteristics of the applied water, such as ponding depth and turbidity and temperature of the water, can also influence the infiltration rate. Ultimately, the infiltration rate is controlled by the least permeable zone within the region of infiltrating water.

Water for the infiltration tests was obtained from a fire hydrant or hose spigot, both supplied by the Industrial Park Well 1 (site number 355224106032801) (fig. 2). The water quality is not likely to be similar to the Rio Grande water that would be applied for the managed aquifer recharge; however, obtaining water of similar quality would have required extraordinary effort. Despite the dissimilar water, the infiltration rates measured by using this water were assumed to be of sufficient quality for the objectives of the characterization.

Double-Ring Infiltration

The double-ring infiltration test is designed to minimize the border or fringe effects of lateral flow. Because the infiltration rate is defined as vertical flow, the outer ring of the double-ring infiltrometer is designed to reduce the lateral flow. The effects of lateral flow decrease with increasing permeability of the sediments (Johnson, 1963). Double-ring infiltration tests were conducted by using two large-volume Mariotte tubes (100,000 milliliters [mL]) that separately fed the inner (12-in. diameter) and outer (24-in. diameter) infiltration rings manufactured by Turf-Tec International (fig. 4*A*). The Mariotte tubes, when used in combination with the 12- and 24-in. infiltration rings, comply with the American Society for Testing and Materials (ASTM) Standard D-3385-03 (Turf-Tec International, 2014). Prior to the start of the test, the infiltration rings are pressed into the ground to a depth of approximately 6 in., after which the rings are filled with a known volume of water and kept at a constant head. The infiltration rings can reportedly measure infiltration in soils with hydraulic conductivities between $1x10^{-6}$ centimeters per second (cm/s), which tend to be clays, and $1x10^{-2}$ cm/s, which tend to be sand-type soils (Turf-Tec International, 2014).

The double-ring infiltration tests were conducted at six locations in ASR-West, five locations in ASR-East, and one location on a Tesuque Formation outcrop (DR-Tesuque), for a total of 12 infiltration tests (fig. 2, table 1). Each of the infiltration tests was run for 1–3 hours. The test was concluded when a constant infiltration rate was reached, as determined by the volume change in the Mariotte tube over time. During the infiltration tests, the depth of water within the infiltration rings was kept constant, ensuring a constant head over the entirety of the test. The depths were checked at 5-minute intervals at the beginning of the test and at 10-minute intervals once the infiltration rate of water began to stabilize. Volume changes within the Mariotte tubes and time intervals were recorded throughout the test. Because these soils were observed to be extremely conductive, most tests were begun after adding approximately 100 gallons of water to the infiltration rings. Often the outer ring had to be supplemented with additional water from a pump to maintain a constant head.

A

B

Figure 4. *A*, double-ring and *B*, bulk infiltration test designs, Pojoaque, New Mexico.

The infiltration rate was determined by dividing the change in water volume, recorded from a calibrated site glass on the Mariotte tubes, by the elapsed time and the area of the corresponding infiltration ring. The water flux in the inner ring was used to calculate the infiltration rate. When the outer ring did not require supplemental water, the water flux for the outer ring was compared with the flux in the inner ring.

Bulk Infiltration

In order to test the infiltration rate of a larger surface area, several falling-head bulk infiltration tests were performed at a selected site in ASR-East (fig. 2). The site of the test was marked off, and trenches for the foundation of a 5- by 5-ft board box were excavated. The trenches were dug to a depth of approximately 5.5 ft, leaving a 5- by 5-ft block of channel deposits between the trenches that were to be tested for infiltration. The 8-ft-tall precut board box was emplaced so that 5.5 ft of the box was below the ground surface, leaving 2.5 ft exposed. Prior to emplacing the wall of the board box, plastic sheeting was set against the exposed side of the test block. As a new side of the test block was exposed, the plastic sheeting was extended, and a new side of the board box was tacked into place. The construction approach avoids disturbing the sediments as best as possible so that the test conditions reflect conditions of naturally deposited sediments. Following the construction of the board box, the outer trench was backfilled with the native material for box stability and access (fig. 4*B*). The falling-head tests were started with 2 to 2.5 ft of head, and the water depth from a staff gage and the elapsed times were recorded manually. Head change at the site was also monitored with a pressure transducer set to record every minute. The pressure transducer was emplaced in a wire-wrapped screen driven approximately 9 in. into the sediments of the test mound.

Static Groundwater Elevations

Groundwater levels from several wells were measured at multiple times during the investigation to determine the directions of groundwater flow by comparing vertical and horizontal hydraulic gradients at the site. Groundwater levels in ASR-East were measured in the existing wells (Pow-Wow and Windmill Wells) and in the two monitoring wells (MW–3 and MW–4) and the two boreholes (BH–3 and BH–4) installed by the USGS in November 2014 (fig. 2, table 1). Groundwater levels were measured by using electric tapes from the top of the well casing or from the land surface for the boreholes. Water levels are available in the USGS National Water Information System (NWIS) (https://doi.org/10.5066/F7P55KJN).

Geochemical Characterization

Groundwater-quality samples were collected from five onsite wells (MW–3, MW–4, Industrial Park Well 1, Pow-Wow Well, and Windmill Well) to assess the potential for regulatory exceedances in naturally occurring groundwater. Groundwater samples were collected by using various pumps. The sample collected from MW–4 was collected by using a Proactive 12-volt submersible pump; the sample collected from MW–3 was collected by using a Grundfos Redi-Flo 2 submersible pump; the samples collected from the Pow-Wow Well and Industrial Park Well 1 were collected by using the existing 5-horsepower pump; and the sample collected from the Windmill Well was collected using a Waterra Hydrolift pump with ¼-in. foot valve. Different pumps were selected on the basis of the well production and method of access.

Groundwater samples were collected as raw and filtered (0.45-micrometer [µm] filters) and preserved as appropriate according to the USGS National Field Manual for the Collection of Water-Quality Data (U.S. Geological Survey, variously dated). The newly installed wells, MW–3 and MW–4, were purged for three well volumes, but because of the low groundwater production, the pumping took place over several days. Measurements of the field parameters pH, temperature, specific conductance (SC), and dissolved oxygen were recorded as wells were purged. The well volumes for the existing wells, Industrial Park Well 1, Pow-Wow Well, and Windmill Well could not be determined because of the lack of construction records; therefore, sampling began when field parameters met stability criteria as defined in the USGS field manual (U.S. Geological Survey, variously dated). Groundwater samples were analyzed in the field for alkalinity and at the USGS National Water Quality Laboratory in Denver, Colorado, for concentrations of the major elements (bromide, calcium [Ca], chloride, F, nitrate [NO_3], magnesium, sodium [Na], potassium, and sulfate [SO_4]) (Fishman and Friedman, 1989; Fishman, 1993); trace elements (aluminum, antimony, As , barium, beryllium, cadmium, chromium, cobalt, copper [Cu], iron [Fe], lead, manganese, nickel, selenium, silver, titanium, vanadium, and zinc); and dissolved solids (DS) (Fishman and Friedman, 1989; Garbarino, 1999; Garbarino and others, 2006). The USGS Reston Stable Isotope Laboratory in Reston, Virginia, analyzed the groundwater samples for the stable isotopes of water, deuterium (δD) and oxygen-18 ($\delta^{18}O$). The stable-isotope ratios are reported in per mil (‰) relative to Vienna Standard Mean Ocean Water (VSMOW) (Révész and Coplen, 2008a; Révész and Coplen, 2008b). Water-quality results are available in the USGS NWIS (https://doi.org/10.5066/F7P55KJN).

Lithologic Descriptions, Elemental Chemistry, Mineralogy, and Slurries

The continuous core was removed from the core barrel and placed into core boxes for description by the site geologist. Five samples from each boring were collected for chemical characterization and bulk mineralogy. Specific conductance and pH were measured on slurries prepared from borehole samples collected at 1-ft intervals. The slurry was prepared by mixing 50 mL of deionized water and 50 grams of soil. After allowing the slurry to equilibrate, the pH and conductivity were measured by using a calibrated Orion 4-star Plus meter with a pH probe and conductivity probe.

Whole-rock analysis was conducted on five core samples from each boring to determine the elemental composition of the sediments and bedrock. RTI Laboratories, Inc., a USGS contract laboratory in Livonia, Michigan, analyzed core samples for inorganic anions, metals, and percent moisture. Inorganic anions were analyzed by ion chromatography by EPA method SW9056S (U.S. Environmental Protection Agency, variously dated), following aqueous extraction of the core samples. Metals were analyzed by inductively coupled plasma-mass spectrometry by EPA method SW6020A (U.S. Environmental Protection Agency, variously dated), following an acid digestion. The percent moisture of each sample was determined gravimetrically by ASTM method D2216-10 (American Society for Testing and Materials, 2010) so that anion and metal results could be reported as dry-weight concentrations in milligrams per kilogram.

Five core samples from each boring were analyzed by the USGS Powder X-Ray Diffraction Laboratory in Denver, Colo. Quantitative mineralogy was calculated by using RockJock (Eberl, 2003), a computer program that determines quantitative mineralogy in powdered samples by comparing the integrated X-ray diffraction (XRD) intensities of individual minerals in complex mixtures to the intensities of an internal standard. Samples were prepared by following the method noted in Eberl (2003), in which materials were crushed to pass through a 250-µm sieve, and then a standard addition of 20 percent corundum was ground with 4 mL of ethanol in a McCrone micronizing mill for 5 minutes. After drying, the mixture was transferred to a plastic scintillation vial with three plastic balls, along with a few drops of Dupont Vertrel, and the vial was shaken again for 10 minutes. The powder was then passed through the sieve again and side loaded into an XRD holder. This procedure produces a randomly oriented sample that is equivalent to that found for a sample prepared by spray drying. Samples were analyzed on a Scintag X-ray Diffractometer from 5 to 65 degrees two-theta by using Cu K-alpha radiation, with a step size of 0.02 degrees two-theta and a count time of 2 seconds per step by using a scintillation counter.

Clay mineral identification was confirmed by XRD scans of a fraction of each sample by using Cu K-alpha radiation. The scans ranged from 2 to 40 degrees two-theta, with a step size of 0.03 degrees two-theta and a count time of 1 second per step by using a scintillation counter. Prior to scanning, the sample was air-dried, ethylene glycolated, and heat treated at 400 and 550 degrees Celsius for 1 hour each.

The hydraulic properties, saturated hydraulic conductivity (K_{sat}), porosity, initial moisture content, and bulk density, were determined on eight selected borehole samples by Daniel B. Stephens and Associates, Inc., in Albuquerque, N. Mex. The K_{sat} was determined by Falling Head, Rising Tail (ASTM method D5084-16) on all the samples but one (American Society for Testing and Materials, 2016). The K_{sat} of the other sample was determined by constant head test (ASTM method D2434-68) (American Society for Testing and Materials, 2006). The porosity, initial moisture content, and bulk density were determined by ASTM method D7263-09 (American Society for Testing and Materials, 2009).

Age-Dating Groundwater Tracers

To provide evidence for the natural recharge mechanisms at the site, age-dating tracers were measured in groundwater samples. Dissolved inorganic carbon (DIC) samples for carbon-13 (^{13}C) and carbon-14 (^{14}C) to carbon-12 (^{12}C) analysis were collected in two 1,000-mL safety-coated glass bottles and sealed with polycone caps. Samples were submitted to the National Ocean Sciences Accelerator Mass Spectrometry Facility at the Woods Hole Oceanographic Institution in Woods Hole, Massachusetts, and analyzed by mass spectroscopy (National Ocean Sciences Accelerator Mass Spectrometry Facility, 2015).

The stable carbon isotope composition delta ^{13}C ($\delta^{13}C$) is a useful indicator of the dissolved inorganic carbon sources in groundwater (Chapelle and Knobel, 1985) because of the different isotopic signatures of carbon dioxide (CO_2), calcite, and other organic constituents that may become part of the dissolved phase in groundwater (for a discussion of the observed ranges of $\delta^{13}C$, see Wang and others, 1998).

Because of its long half-life, the amount of ^{14}C in the DIC may be used to estimate groundwater ages ranging from 1,000 to about 30,000 years before present (Clark and Fritz, 1997). Carbon-14 has a half-life of 5,730 years and is produced in the upper atmosphere by the interaction of cosmic rays and atmospheric nitrogen. The cosmogenic ^{14}C is rapidly oxidized and becomes incorporated into biologic and hydrologic processes as carbon dioxide ($^{14}CO_2$) (Plummer and others, 2012).

The ^{14}C concentrations in this investigation are reported as the non-normalized percent modern carbon. Percent modern carbon, not normalized for ^{13}C fractionation, is defined as the ratio of ^{14}C to ^{12}C of the sample divided by the standard ^{14}C to ^{12}C ratio of the National Bureau of Standards oxalic acid in 1950 and multiplied by 100 (Plummer and Glynn, 2013). The ^{14}C concentration, normalized for ^{13}C fractionation, is commonly reported by radiocarbon labs, and the normalized ^{14}C activities can be converted back to non-normalized activities with the following equation (Mook and van der Plicht, 1999):

$$^{14}a^{S} = {}^{14}a_{N}\left[\frac{\left(1+{}^{13}\delta\right)}{0.975}\right]^{2}\exp\left[\frac{-\left(y-1,950\right)}{8,267}\right], \qquad (1)$$

where

$^{14}a^{S}$ is the ^{14}C activity ratio (expressed in percent modern carbon) of the sample at the time of sample collection,

$^{14}a_{N}$ is the commonly reported normalized ^{14}C activity ratio (expressed in percent modern carbon),

$^{13}\delta$ is the $\delta^{13}C$ of the DIC (in per mil),

exp exponential function

y is the year of sample collection or year of analysis, and

8,267 is $1/\lambda$, and λ is the ^{14}C decay constant ([ln 2])/5,730).

The non-normalized ^{14}C values were used to calculate an unadjusted radiocarbon age ($t_{unadj.}$) in years before present relative to 1950. The unadjusted radiocarbon age is determined by the following equation (Plummer and others, 2012):

$$t_{unadj.} = \left(\frac{5,730}{\ln 2}\right)\ln\left(\frac{A_0}{A}\right) - \left[\frac{\left(y-1,950\right)}{1.029}\right], \qquad (2)$$

where

5,730 is the modern half-life of ^{14}C,

A_0 is the initial ^{14}C content (in percent modern carbon), and

A is the measured ^{14}C content (in percent modern carbon) in the sample.

For this investigation, the radiocarbon age is reported as the unadjusted age, with A_0 assumed to be 100 percent modern carbon (pmC). The possible effects of geochemical reactions on the initial ^{14}C content measured in the groundwater samples are discussed conceptually in this report, but the lack of clearly defined flow paths prohibited the accurate use of geochemical modeling for adjusting radiocarbon age.

Tritium (^{3}H) is a radioactive isotope of hydrogen that is short-lived, with a half-life of 12.32 years (Lucas and Unterweger, 2000). During the late 1950s to the mid-1960s, testing of nuclear weapons raised the atmospheric concentrations of ^{3}H hundreds of times above the normal background concentrations (Plummer and Friedman, 1999). In 1963, the Nuclear Test Ban Treaty was signed, eliminating most of the aboveground nuclear weapons testing in the world. Since then, ^{3}H levels in the atmosphere have decreased to natural levels. The higher ^{3}H concentrations from nuclear weapons testing continue to be present in some groundwater and may be used qualitatively to constrain the recharge date (Clark and Fritz, 1997). In the atmosphere, ^{3}H is rapidly oxidized and enters the hydrologic cycle, making it a valuable tracer for groundwater that has recharged since the 1950s. The ^{3}H concentration in precipitation is not influenced by temperature (as are oxygen-18 [$\delta^{18}O$] and deuterium [δD]), and the only fractionation is due to evaporation following precipitation, where ^{3}H is fractionated at about twice the extent of δD (Bolin, 1958). Fractionation is the enrichment of one isotope relative to another in the reactant or product of a chemical or physical process. Evaporative fractionation of ^{3}H would affect the apparent age differently depending on whether the age was determined to be before or after the peak atmospheric concentrations in 1963. If the apparent age were interpreted as after 1963, the enrichment of ^{3}H through evaporation would bias the apparent age older than the actual age when the water infiltrated. If the apparent age is interpreted as before 1963, the age would be biased younger than the actual age.

Tritium samples were collected in two 500-mL high-density polyethylene bottles and sealed with polycone caps. Samples were submitted to the University of Miami Tritium Laboratory in Miami, Florida, for analysis. The ^{3}H activity was determined by gas proportional counting, following low-level enrichment (University of Miami Tritium Laboratory, 2016). Tritium activity is reported in tritium units (TU), in which 1 TU is defined as one atom of ^{3}H in 10^{18} atoms of hydrogen.

Quality Assurance

To assess the quality of the laboratory data for major ions, the anion and cation data were evaluated for ion electrical balance. The differences between the milliequivalents of anions and cations for the six samples were all within 5 percent.

Replicate samples were collected for all analytes at well MW–3. The relative percent difference (RPD) between the two samples' concentrations was used to determine the variability in the samples.

$$RPD = 100\frac{\left(\text{larger result} - \text{smaller result}\right)}{\left(\text{larger result} - \text{smaller result}\right)/2}, \qquad (3)$$

The RPD for values of all analytes in the replicate samples was within 10 percent, with the exception of Fe (68 percent) and NO_3 (11 percent). No blanks were collected because of the use of multiple pumps and dedicated equipment. Because there were no blanks collected, the effect of contamination on the major and trace elements results from the pumps or fittings could not be verified.

Hydrogeologic and Geochemical Characterization and Evaluation

The data collected as part of this investigation are presented in the following sections. The data are evaluated with respect to the potential suitability of these two arroyos as sites for managed aquifer recharge through surface infiltration.

Potential for Conveyance of Managed Flows

The geometries of the channels in both arroyos are braided, and the thalweg and bankfull heights are irregular. The average slope in ASR-East is 3.5 percent to the north, with a maximum slope of 10.0 percent. The average slope in ASR-West is 3.0 percent to the north, and the maximum slope is 9.2 percent. The channels are flanked by hills with gradually increasing slopes, and the channels' shapes vary from a saw-tooth geometry with multiple channels to a single well-defined channel. On the basis of the irregular channel geometries, it was determined that the two reaches are not suitable for gaging surface flow or using indirect methods to estimate flows.

HEC-RAS version 4.1 (U.S. Army Corps of Engineers, 2010) was used to compute water-surface profiles for several discharges to estimate the flow, velocities, and depths at which the reaches were mostly submerged (that is, bankfull). The braided-channel conditions and the inflow of many small tributaries along both reaches complicated the water-surface profile computations. The water-surface profiles were evaluated by using three different upstream boundary conditions (critical depth, 1 ft below critical depth, and 2 ft below critical depth). The use of supercritical conditions in the model is considered to be reasonable given that the average gradients for both reaches are equal to or greater than 3 percent (ASR-West, 3.0 percent; ASR-East 3.5 percent). Convergence for a majority of the downstream cross-sections was only achieved in both arroyos at flows greater than 2,000 ft^3/s. Above 2,000 ft^3/s, streamflow begins to overflow the thalweg and flow through the parallel channels.

The water-surface profile for the ASR-West reach for a flow of 2,000 ft^3/s was computed with eight cross-sections, spaced approximately 250 ft apart, in a 2,100-ft segment. A single weighted-average Manning's roughness coefficient based on the overall channel conditions was used to compute the water-surface profile at each cross-section. The weighted-average Manning's roughness coefficients for the ASR-West cross-sections ranged from 0.032 to 0.035 (table 2). Manning's roughness coefficient values were assigned on the basis of the channel morphology, channel substrate, and overbank vegetation (Aldridge and Garrett, 1973). A Manning's roughness coefficient of 0.030 was assigned to the channel bottom. The Manning's roughness coefficient was slightly increased to 0.032 in parts of the channel where there were grass and small shrubs. In the left and right overbank areas and in portions of the channel where Piñon trees and brush were present, a Manning's roughness value of 0.045 was used.

The computed water surface showed divided flow conditions in all cross-sections in ASR-West (table 2). The velocity in the cross-sections ranged from 6.43 feet per second (ft/s) to 11.70 ft/s, and the average velocity was 8.84 ft/s. The hydraulic depths in the cross-sections ranged from 0.77 ft to 1.62 ft, and the average hydraulic depth was 1.12 ft.

The water-surface profile for the ASR-East reach for a flow of 2,000 ft^3/s was computed from 11 cross-sections, spaced approximately 250 ft apart, in a 2,700-ft segment. The weighted average Manning's roughness coefficients for the ASR-East cross-sections ranged from 0.030 to 0.035 (table 2). The velocity in the cross-sections for a discharge of 2,000 ft^3/s ranged from 8.14 ft/s to 15.64 ft/s, and the average velocity was 10.07 ft/s. The hydraulic depth in the cross-sections ranged from 0.55 ft to 2.05 ft, and the average hydraulic depth was 1.18 ft.

These computed water-surface profiles should be considered to have a very high level of uncertainty because the water surfaces could not be verified with high-water marks. As expected with the braided channel conditions, there was large variability in the velocity in each cross-section. To account for the braided nature of both reaches, ineffective flow areas could have been designated in each cross-section; however, without any information about the timing of the tributary inflows, ineffective flow areas were not designated, and it was assumed that the discharge was constant in both reaches.

The calculated discharges that would result in overbank flows were greater than 2,000 ft^3/s and greatly exceeded those potentially to be used for managed recharge. (The PBRWS is being designed to provide a minimum of 4,000 acre-ft per year [~5.6 ft^3/s, HKM Engineering, 2008], far less than the channel capacity.) Evaluation of channel geometry and computed water-surface profiles indicates that the channel capacity is favorable for managed recharge.

Aquifer Storage Capacity

The aquifer storage capacity was evaluated by estimating the volume of channel sands in each arroyo from the surface geophysics. The descriptions of the subsurface lithology were used to qualitatively assess the water-storage potential of the channel sands and underlying bedrock.

Table 2. Location and description of cross sections used in water-surface computations of bank-full conditions in two arroyos near Pojoaque, New Mexico.

[NAD 83, North American Datum of 1983; NAVD 88, North American Vertical Datum of 1988; Manning's n, Manning's roughness coefficient; ft/s, foot per second; ft, foot; ASR, aquifer storage and recovery; X, cross-section]

Site name	Thalweg location			Average Manning's n	Velocity (ft/s)	Depth (ft)	Description
	Latitude	Longitude	Elevation				
	NAD 83		ft NAVD 88				
ASR-East							
X13	35.86227	-106.04285	6,050.0	0.031	8.14	2.05	Most upstream cross section
X12	35.86262	-106.04277	6,046.0	0.032	15.64	1.22	
X11	35.86311	-106.04299	6,040.0	0.032	8.24	1.06	
[1]X10	35.86310	-106.04300	6,040.0				Not used in water-surface computation
X9	35.86339	-106.04299	6,035.9	0.031	8.7	1.28	
X8	35.86374	-106.04300	6,031.9	0.035	9.67	1.06	
X7	35.86586	-106.04313	6,004.1	0.030	10.45	1.42	Divided flow
[1]X6	35.86739	-106.04383	5,983.9				Not used in water-surface computation
X5	35.86770	-106.04383	5,980.0	0.032	9.96	1.09	
X4	35.86850	-106.04407	5,969.2	0.032	8.39	1.15	Divided flow
X3	35.86870	-106.04416	5,966.0	0.031	11.87	0.96	Divided flow
X2	35.86909	-106.04430	5,960.6	0.030	8.3	1.16	Divided flow
X1	35.86967	-106.04443	5,953.4	0.032	11.5	0.55	
ASR-West							
X9	35.86402	-106.05482	5,942.5	0.032	6.43	1.17	Divided flow, most upstream cross section
X8	35.86415	-106.05575	5,936.7	0.032	11.70	1.23	Divided flow
X7	35.86535	-106.05542	5,928.6	0.032	7.32	1.05	Divided flow
X6	35.86607	-106.05600	5,919.0	0.033	7.78	0.77	Divided flow
X5	35.86630	-106.05613	5,915.5	0.032	7.44	1.20	Divided flow
X4	35.86718	-106.05699	5,902.8	0.034	10.02	1.03	Divided flow
X3	35.86822	-106.05741	5,890.1	0.032	9.40	1.62	Divided flow
X2	35.86868	-106.05796	5,884.8	0.035	10.63	0.92	Divided flow
[1]X1	35.86911	-106.05833	5,880.6				Not used in water-surface computation

[1]Not used in water-surface computation because model did not converge because of large changes in channel area.

Surface Geophysics

The inverse modeling results of the 2-D DC resistivity data are shown for each arroyo in figure 5. The DC resistivity survey was very effective at imaging the contact between coarse sand (resistivity above 70 ohmmeters [ohm-m]) in the arroyo channel and the bedrock (resistivity below 20 ohm-m). The electrical conductivity of the bedrock was too high to effectively image any subtle structures, such as preferential groundwater pathways. Because of the overall high conductivity of the bedrock, the water table could also not be accurately imaged in either of the arroyos.

There are areas beneath each arroyo where the thickness of the coarse channel sand fluctuates. Figure 5*A* shows that the coarse channel sands (shown in pink) of ASR-East along the longitudinal line are thickest on the southern end of the profile. The coarse channel sands imaged in the perpendicular transects are observed to be centered about the longitudinal line in ASR-East and show similar thicknesses and widths throughout the survey extent. The thickness of the coarse channel sands in the perpendicular lines correspond well with the thickness in the longitudinal lines in both arroyos.

ASR-West shows similar fluctuations in the thickness of the coarse channel sands along the longitudinal line (fig. 5*B*), but the overall thickness of coarse channel sands is thinner in ASR-West than in ASR-East. The perpendicular transects in ASR-West show that the thicknesses and widths of the resistant channel sands are greater towards the north. Unlike ASR-East, the coarse channel sands imaged in the perpendicular lines of ASR-West seem to be off-center from the longitudinal line. Figure 5*B* shows that the thickest parts of the coarse channel sands tend to be north and east of the present day arroyo channel.

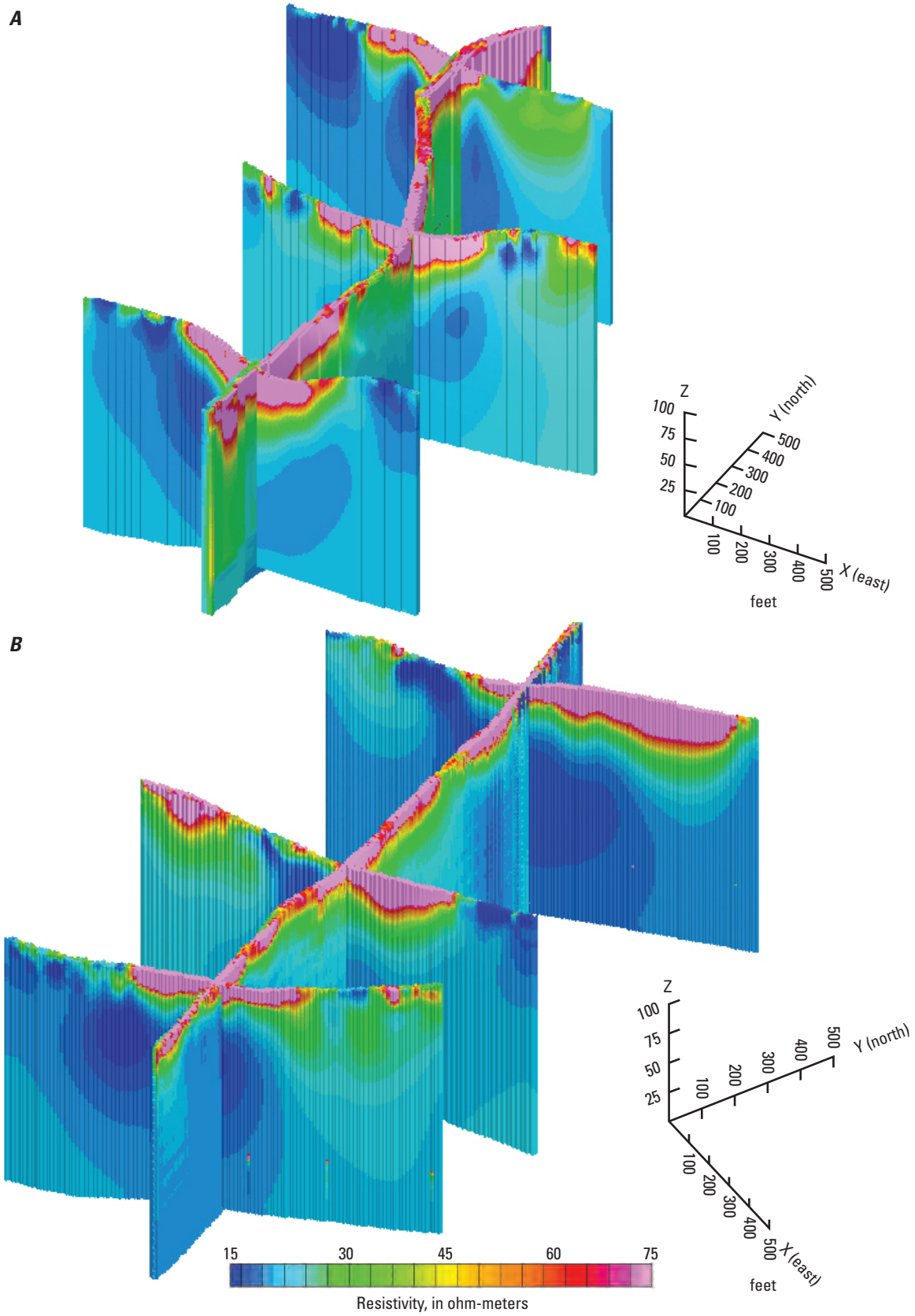

Figure 5. The direct-current resistivity data collected along *A*, Aquifer Storage and Recovery (ASR)-East and *B*, ASR-West near Pojoaque, New Mexico.

The inverse modeling results of the FDEM soundings are shown overlapping the DC resistivity profiles in figure 6. Figure 6 shows the FDEM data for each arroyo clipped to show only values above 70 ohm-m. The FDEM technique effectively imaged the coarse channel sands in each of the arroyos but was not able to image the water table because of the highly conductive bedrock. The inversion data from ASR-East (fig. 6*A*) were very low in environmental noise, and the resulting 3-D grid correlates well with observations in the DC data. As seen in the DC data, the thickness of the resistive channel sands is greatest on the southern end of the study area, and there are similar areas where the coarse sands thin out completely. The FDEM data also compare well to the DC survey in that the overall east-west extent remains consistent and centered along the arroyo.

The FDEM data from ASR-West (fig. 6*B*) were much noisier (poor quality) and needed much more manual manipulation to show the results. A nonlinear filter was applied to the inversion results, and much less stringent gridding parameters were used. The results do not correlate particularly well to the results of the DC resistivity survey and are much less robust than the FDEM results of ASR-East. The resistive feature shown in the FDEM data best compares (in thickness and extent) to the DC survey on the southern end of the study area. Unlike the DC results, the FDEM results place the resistive feature to the west of the center longitudinal line on the north end of the study area. This difference is likely an artifact of the poor-quality data, and thus the results are not considered as robust as those of the DC survey.

The surface geophysics interpretations indicate that the channel sands are generally between 30 and 50 ft thick at ASR-East and slightly thinner at ASR-West. FDEM and DC electrical resistivity surveys indicate that the deepest part of the sands at ASR-East is beneath the center of the present channel. The DC survey indicates that the deepest sands at ASR-West are slightly east of the center of the current channel. Assuming equal porosities, there is more storage potential for water in the sands of ASR-East than in ASR-West. Rough estimates of the bulk volume of the unconsolidated channel sands underneath each reach based on the mean resistivity of the FDEM geophysics are about 410 acre-feet (acre-ft) (501,000 cubic meters [m^3]) at ASR-East and about 190 acre-ft (236,000 m^3) at ASR-West (table 3). Assuming a typical porosity for sands of 40 percent (Argonne National Laboratory, 2015), there is probably less than 300 acre-ft of storage potential in the channel sands of the two reaches. Based on the PBRWS-estimated need to supply 1,200 gal/min (50 percent of the average daily water-use requirement; HKM Engineering, 2008), the channel sands could provide about 45 days of peak withdrawal without any recharge.

Subsurface Lithology

The unconsolidated channel sands, terrace deposits, and the underlying bedrock were characterized by descriptions of the continuous core and analysis of core samples. The unconsolidated material overlying the bedrock in the channel is generally described as tan to light brown and occasionally reddish brown. Silts and fine sands were interspersed with very coarse sands and gravels and occasional cobbles and boulders. Silty clays were partially competent and present as thin (less than [<] 24 in.) sections. The sands and gravels were rounded to angular and appeared to be composed primarily of quartz, feldspar, and darker mafic minerals. Variable amounts of carbonate precipitation were observed by the slight to strong reactions with 5 percent hydrochloric acid. The unconsolidated material at the two monitoring well sites, which are on the terrace hillside adjacent to the channel, was primarily silts and sands with occasional coarse sands and gravels, suggesting alternating alluvial deposits from overland wash and mass wasting of the hillside and eolian deposition. In comparison, the unconsolidated material within the channel tended be larger and more rounded, indicating a higher energy depositional environment. There were small sections of unconsolidated material in the hillslope borings that looked very similar to the channel sands, suggesting the migration of the channel location over time.

The bedrock is generally described as fine grained and tan to light brown, with varying degrees of cementation and moisture. Tan to light brown sections of sandstone and siltstones were generally less than 6 in. thick. Sections with finer grained zones tend to be reddish brown and grayish tan. The cores, which were dominated by clay, would expand up to 2 in. per foot when brought to the surface.

The influence on groundwater conditions of the interbedded fine-grained deposits and coarser sandstones and siltstones in the Tesuque Formation is highlighted in the quasi-artesian conditions and areas of perched saturation. For instance, artesian conditions were observed while drilling at the MW–4 location; the saturation was observed at 73.5 ft bls while collecting core but rose to 53.75 ft bls in the borehole the following day. The interbedded layers of gravel, sand, silt, and clay observed in this investigation support earlier descriptions of the Tesuque Formation and suggest that the overall aquifer is composed of individual permeable units that may have limited connectivity to shallower or deeper units.

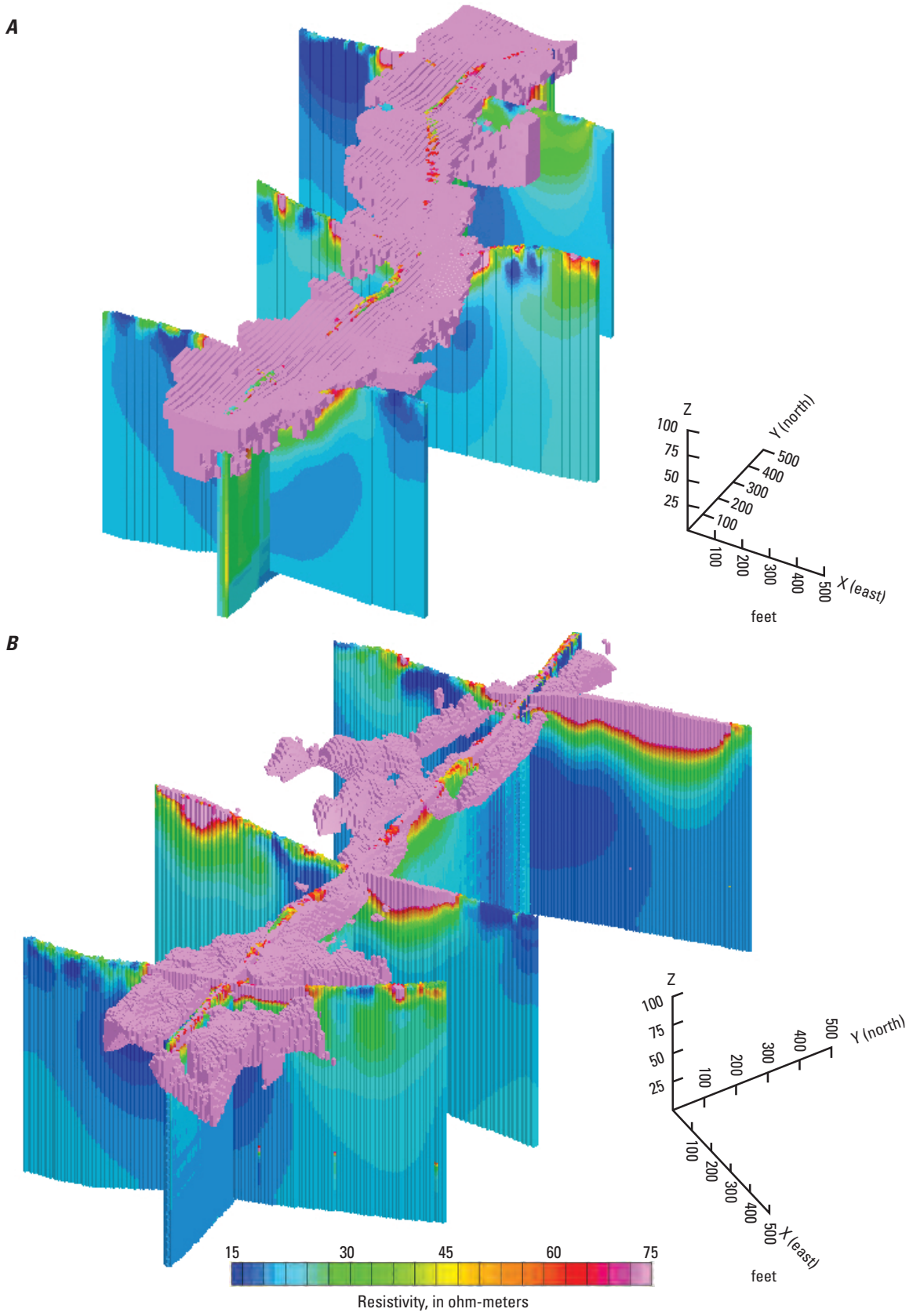

Figure 6. The frequency-domain electromagnetic data collected along *A*, Aquifer Storage and Recovery (ASR)-East and *B*, ASR-West near Pojoaque, New Mexico.

Table 3. Approximate volume of channel sands for two study reaches, Pojoaque, New Mexico.

[The frequency domain electromagnetic resistivity values for each 3D volume are selected as the mean resistivity value for the area selected to represent channel sands, plus or minus one standard deviation (σ). There is a 68-percent confidence the volume of sands lies between the upper and lower bounds. σ, standard deviation; ohm-m, ohm-meter; m^3, cubic meter; %, percent]

ASR-East			
Total model volume (acre-feet)		**2,130.69**	
	-σ	**Mean**	**σ**
Resistivity (ohm-m)	67.61	109.65	177.83
Bulk volume (m^3)	1,094,943	501,174	159,341
Bulk volume (acre-feet)	887.68	406.31	129.18
Percent of total volume (%)	41.66	19.07	6.06

ASR-West			
Total model volume (acre-feet)		**1,163.93**	
	-σ	**Mean**	**σ**
Resistivity (ohm-m)	43.65	89.13	181.97
Bulk volume (m^3)	724,927	236,351	69,334
Bulk volume (acre-feet)	587.71	191.61	56.21
Percent of total volume (%)	50.49	16.46	4.83

Descriptions of the samples collected from the cores, the clay content, and the relation of the samples to the bedrock contact and static water levels are reported in table 4. The hydraulic properties of selected samples are reported in table 5.

On the basis of the observations made during drilling and the descriptions of the cores, the geophysical interpretations of the contact between the unconsolidated channel sands and the resistive bedrock were confirmed. The coarse-grained deposits of the channel sands appeared to be very permeable and well-connected despite the occasional fine-grained clay lenses. The semiconfined conditions observed in the bedrock borings and the presence of expanding clays suggest limited effective storage in the bedrock. The lithology of the channel sands is favorable to managed recharge, but the small volume of the sands places limits on the water-storage potential. Although groundwater was found in the bedrock, the prevalence of the fine-grained deposits limit the effective storage of applied water and suggest that recharge of more permeable layers may only occur on the outcrops or where those layers subcrop in the channel bottom.

Evaluating the Potential for Recharge through Surface Infiltration

The potential for recharging the aquifer through surface infiltration was evaluated by measuring the infiltration rate of the streambed deposits, measuring and comparing the shallow groundwater elevations with the deep groundwater elevations, and examining stable isotopes and age-dating tracers in the groundwater for evidence of local recharge.

Streambed Infiltration Rate

Infiltration rates in the stream channel were determined by using double-ring and bulk infiltration tests (fig. 2). The infiltration tests were performed on a variety of channel morphologies, from the thalweg to vegetated sand bars. Results from the double-ring infiltration tests ranged from 9.7 to 94.5 feet per day (ft/d) (12.3 to 120 centimeters per hour [cm/hr]) (table 6). The average infiltration rate was 34.5 ft/d (43.8 cm/hr), and the median value was 22.7 ft/d (28.8 cm/hr). These rates are above the highest rate of 9.9 ft/d (12.6 cm/hr) reported by Johnson (1963) for gravelly silt loam.

In order to test the infiltration rate of a larger surface area, seven falling-head bulk infiltration tests were performed at a selected site in ASR-East (fig. 2). The infiltration rates measured at the site were between 57.6 and 60.5 ft/d (73.2 and 76.8 cm/hr; table 6). This rate was higher than rates reported for other ephemeral channels near the Rio Grande. The bulk infiltration rates measured at two sites in Bear Canyon Arroyo in Albuquerque, N. Mex., were 11.3 and 25.2 ft/d (14.4 and 32 cm/hr) (Bob Marley, Daniel B. Stephens & Associates, Inc., written commun., March 27, 2015). The infiltration rate in the Santa Fe River near La Bajada, N. Mex., was determined to be 2.7–10.5 ft/d (6.9–26.7 cm/hr) by streamflow loss (Thomas and others, 2000).

Although a detailed assessment of the infiltration rate of the Tesuque Formation is beyond the scope of this investigation, one double-ring infiltration test was performed on an outcrop of the Tesuque Formation to estimate the infiltration rate of the bedrock underlying the channels. The result of the test was 4.3 ft/d (5.5 cm/hr; table 6), comparable to the results of an infiltration test on silt loam soil reported by Johnson (1963). Although this infiltration rate is less than the rate measured in the channel sands, it was measured on the outcrop of the Tesuque Formation and should be regarded as the high end of potential infiltration rates for the bedrock underlying the channel. This consideration is due to the degradation of the structure and increased secondary permeability that is thought to occur with exposure to weathering at land surface (Jury and others, 1991).

Table 4. Summary of sample depths, bedrock depths, static water level, clay content, and non-clay mineralogy in four borings, Pojoaque, New Mexico.

[mm, month; dd, day; yyyy, year; ft, foot; bls, below land surface; %, weight percent; $CaCO_3$, calcium carbonate; tr, trace]

Date (mm–dd–yyyy)	Depth (ft bls)	Description	Clay content (%)[1]	Nonclays (%)[1]					
				Quartz	K-feldspar	Plagioclase	Calcite	Clinoptilolite (Hector)	Total nonclays
		MW-4 355152106023801							
11–16–2014	12–13	Unconsolidated, medium to very coarse sands with gravels directly above contact.	0.0	43.9	19.4	35.4	1.0	0.0	99.7
		Bedrock = 13.5 ft bls							
11–16–2014	36–37	Fine sand and silt. First depth of noticeable moisture.	15.0	44.4	14.7	15.6	5.2	5.1	85.0
		Static depth to water = 53.75 ft bls							
11–16–2014	54–55	Moderately consolidated fine sand/silt present.	20.0	49.9	15.8	13.8	0.0	tr	79.5
11–16–2014	74–75	Top of saturated silty clay layer.	23.5	36.3	14.2	11.3	12.9	1.8	76.5
11–16–2014	86–87	Zone of increasing sand content and water.	14.8	40.7	15.9	21.7	3.6	2.9	84.8
		MW-3 355208106024201							
11–22–2014	13.5–14.5	Unconsolidated coarse sands and gravels.	8.0	38.9	21.1	25.6	6.5	0.0	92.0
		Bedrock = 14.5 ft bls							
11–22–2014	42–43	Fine sandstone/siltstone with $CaCO_3$ deposition and some water content.	44.4	12.9	6.5	4.2	31.3	0.6	55.4
11–22–2014	93–94	Weakly to moderately consolidated with fine sand/silt with some clay.	16.2	48.4	14.2	16.5	3.7	0.0	82.9
		Static depth to water = 109.55 ft bls							
11–22–2014	114.5–115.5	Loosely to moderately consolidated fine to medium sand. Beginning of water.	11.5	51.0	14.3	18.1	2.9	2.4	88.7
11–22–2014	123–124	Bottom of core.	27.4	39.4	12.3	15.5	3.3	2.1	72.6
		BH-4 355147106023501							
11–13–2014	19–20	Unconsolidated sand.	2.0	42.3	22.8	32.4	0.5	0.0	98.0
11–13–2014	28–29	Gray clay zone.	45.6	27.5	11.3	10.5	3.1	1.6	54.1
11–13–2014	30–31	Slightly consolidated sand with iron oxide staining below 2 ft sandy clay plug.	2.6	41.7	21.9	32.9	0.8	0.0	97.4
11–13–2014	50–51	Unconsolidated material above sandy clay zone.	11.3	36.6	20.1	30.3	1.8	0.0	88.7
		Bedrock = 51.25 ft bls							
11–13–2014	56–57	Consolidated coarse-grained material within silty-sand clay zone.	3.7	31.0	12.2	24.7	28.0	tr	95.9
		Static depth to water = 58.3 ft bls							
		BH-3 355207106024001							
11–19–2014	10–11	Loosely to moderately consolidated coarse sands and gravels.	2.6	39.7	25.2	30.6	1.8	0.0	97.4
11–19–2014	20–21	Medium to very coarse with sands and gravels, $CaCO_3$ cementation.	2.6	42.3	19.3	33.5	2.5	0.0	97.4
		Bedrock = 24 ft bls							
11–19–2014	24–25	Top of contact. Fine grained.	11.2	47.5	17.7	19.1	4.1	tr	88.5
11–19–2014	47	Coarse sand facies within finer grained formation. First fully saturated zone.	3.1	43.0	22.2	28.8	2.4	0.0	96.6
		Static depth to water = 49.1 ft bls							
11–19–2014	60–61	Fully saturated, fine-grained silty clay at total depth.	40.9	23.7	11.2	9.0	14.3	0.9	58.2

[1]Mineral identifications and proportions are from XRD analysis.

Table 5. Hydraulic properties of selected samples from borings, Pojoaque, New Mexico.

[ft, foot; bls, below land surface; %, percent; g/cm^3, grams per cubic centimeter; cm/s, centimeter per second; cm/hr, centimeter per hour; E, scientific notation]

Site name	Description	Depth interval (ft bls)	Moisture (%)	Dry bulk density (g/cm^3)	Wet bulk density (g/cm^3)	Calculated porosity (%)	Saturated hydraulic conductivity	
							(cm/s)	(cm/hr)
BH-4	unconsolidated deposits	29.0–29.5	9.4	1.56	1.7	41.3	2.97E-04	1.07
BH-4	unconsolidated deposits	45.0–45.5	3.5	1.70	1.76	36	9.94E-05	0.36
MW-4	bedrock	21.5–22.0	3.5	1.64	1.7	37.9	1.85E-05	0.07
BH-3	unconsolidated deposits	12.0–12.5	1.2	1.88	1.9	29.1	2.33E-02	83.88
BH-3	bedrock	25.5–26.0	7.3	1.61	1.73	39.3	2.55E-04	0.92
BH-3	bedrock	42.5–43.0	7.9	1.69	1.82	36.2	4.59E-04	1.65
MW-3	bedrock	55.5–56.0	10.5	1.56	1.73	41.1	1.60E-05	0.06
MW-3	bedrock	92.5–93.0	11.7	1.56	1.74	41.3	7.37E-04	2.65

The high infiltration rates in the arroyos suggest that only large, intense precipitation events would result in surface runoff. Although horizontal hydraulic conductivity cannot be derived from the vertical infiltration rates measured, the high infiltration rates measured in the channel suggest that the vertical and horizontal conductivities are quite high; therefore, it is plausible to imagine water infiltrating into the channel sands and running along the bedrock contact and out of the reach instead of infiltrating into the bedrock. This idea is supported by the lack of water observed in either the alluvium or the shallow bedrock despite a large rain event that occurred about 1 month prior to the investigation. The large monsoon storm produced enough runoff to carry sediment and debris onto New Mexico Highway 502, approximately 1 mi downstream from the study reaches.

The product of the estimated surface area of the channels and the median infiltration rate calculated for the channel sands was used to estimate the rate at which water could be applied for recharge to the unconsolidated channel-bed material without producing surface flows downstream of the reach. On the basis of the survey of both channels, an average width of 10 ft was assumed for the 2,500-ft length of each reach. By using the median infiltration rate of 22.7 ft/d, the application rate would be slightly less than 6.6 ft^3/s (2,960 gal/min). Assuming 40 percent porosity and using the estimated volume of the channel sands from the geophysical survey, it would take approximately 12 days to fill the ASR-East arroyo at 6.6 ft^3/s, assuming no losses from flow out of the reach or to the surrounding bedrock or evapotranspiration (ET). Assuming the same application rate in ASR-West, it would take just under 6 days to fill the unconsolidated material in that reach. The estimated application rate (6.6 ft^3/s) for managed flows is favorable for managed recharge because the rate is approximately 2.5 times higher than the estimated average withdrawal rate of 2.7 ft^3/s (1,200 gal/min) and far lower than the channel capacity for flood flows estimated from the water-surface profile calculations (2,000 ft^3/s).

Static Groundwater Elevations

Groundwater elevations of boreholes and wells completed at various depths were measured to determine the direction of groundwater-flow paths and local vertical gradients (tables 4 and 7). There are no construction records to verify the depths of the existing wells, but the Pow-Wow Well is at least 235 ft deep on the basis of the total depth achieved with an electric tape. The depth of refusal for the electric tape was likely due to interference by part of the pump assembly, and therefore it is assumed that the well is deeper. The Industrial Park Well 1 is thought to be around 800 ft deep, according to local utility personnel (Alan Martinez, Pojoaque Utilities, oral commun., 2014). The groundwater elevations in ASR-East are plotted with the linear distance from BH–4 to the Pow-Wow Well in figure 7.

The groundwater elevation profile indicates a hydraulic gradient in the direction of the stream channel that generally follows the local topography. This local gradient differs from reports that the regional groundwater flow in the study area is west-northwest from the Sangre de Cristo Mountains to the Rio Grande (McAda and Wasiolek, 1988; Anderholm, 1994, Manning, 2008). The northerly gradient in the groundwater elevations at the site is likely the result of local recharge that flows down and towards the Pojoaque River. The discharge point of the shallow groundwater was not determined. There are no known springs in the area, and therefore the shallow groundwater is thought to discharge to the Pojoaque River groundwater system or down to the deeper aquifer units.

The groundwater gradient between the shallow wells and boreholes, and those wells screened deeper in the Tesuque Formation, indicates that the groundwater in the shallow aquifer units has the potential to migrate to deeper units (fig. 7, table 7). This downward gradient is most likely to result from local recharge of the shallow groundwater by precipitation. The ability for local recharge to occur from precipitation is favorable to managed recharge because it indicates an existing pathway for surface water to reach the aquifer units underlying the channel.

Table 6. Double-ring and bulk infiltration rate test results, Pojoaque, New Mexico.

[mm, month; dd, day; yyyy, year; cm/hr, centimeter per hour; ft/d, foot per day; NAD 83, North American Datum of 1983; NAVD 88, North American Vertical Datum of 1988; °C, degree Celsius; ASR, aquifer storage and recovery; DR, double ring; n/r, not recorded; *, several tests performed during the day]

Site name	Date (mm–dd–yyyy)	Time	Infiltration rate		Latitude	Longitude	Elevation	Water parameters		Soil temperature	Description
			(cm/hr)	(ft/d)	NAD 83		feet NAVD 88	Temperature (°C)	pH	(°C)	
ASR-East											
DR East 4	10–29–14	10:00	28.8	22.7	35.866087	-106.043062	6,002.3	n/r	8.6 to 8.7	15.2	A vegetated sandbar in middle of reach
DR East 5	11–03–14	10:45	41.1	32.4	35.863772	-106.042921	6,031.8	17.0 to 17.9	8.7 to 8.9	n/r	Mid-channel at top quarter of reach
DR East 6	11–03–14	14:10	12.3	9.7	35.866949	-106.043505	5,991.5	16.9 to 17.6	8.6 to 8.7	n/r	Out of the thalwag with possible sheeting flows in middle of reach
DR East 7	11–04–14	9:37	14.4	11.3	35.869594	-106.044116	5,955.7	12.2 to 15.1	8.5 to 8.7	n/r	Mid-channel at bottom of reach
DR East 8	11–04–14	13:28	16.5	13.0	35.865746	-106.042924	6,007.2	16.5 to 17.6	8.5 to 8.7	n/r	Out of the thalwag, in middle of reach
Bulk[1]	03–10–15	*	76.8	60.5	35.867563	-106.044078	5,981.6	9.4 to 9.7	8.7 to 8.8	6.0	Mid-channel at bottom of reach
Bulk[1]	03–11–15	*	73.2	57.6	35.867563	-106.044078	5,981.6	8.7 to 8.9	8.7 to 8.8	5.6	Mid-channel at bottom of reach
ASR-West											
[1]DR West 1	10–30–14	9:00	91	72	35.865221	-106.055611	5,931.1	n/r	n/r	n/r	Sandbar at top quarter of reach
DR West 2	10–30–14	15:00	65.8	51.8	35.866467	-106.056347	5,913.1	21.3 to 21.6	8.7 to 7.8	16.5	Right-bank in middle of reach
DR West 3	10–31–14	9:30	65.8	51.8	35.867892	-106.057330	5,894.0	16.5 to 16.8	8.7 to 8.9	n/r	Mid-channel in bottom third of reach
DR West 4	10–31–14	13:00	13.2	10.4	35.868991	-106.058419	5,881.6	16.5 to 17.1	8.7 to 8.8	n/r	Mid-channel near converging tributaries at bottom of reach
DR West 5	11–05–14	9:15	120	94.5	35.865328	-106.055690	5,930.1	11.2 to 11.5	8.7 to 8.9	n/r	Sandbar at the top quarter of reach
DR West 6	11–05–14	12:10	12.3	9.7	35.866054	-106.056120	5,920.3	16.4 to 17.8	8.7 to 8.9	n/r	Out of the thalwag, at bottom third of reach
Tesuque Formation outcrop											
Tesuque	11–06–14	15:45	5.5	4.3	35.872236	-106.055438	5,921.9	13.4 to 13.9	8.7 to 8.8	5.8	Tesuque outcrop on hill slope

[1]Infiltration rate determined by falling-head.

Table 7. Water-level elevations for wells and field parameters for groundwater and surface-water samples near the study area, Pojoaque, New Mexico.

[mmHg, millimeter of mercury; temp, temperature; °C, degree Celsius; O_2, oxygen; mg/L, milligram per liter; µS/cm, microsiemen per centimeter; NTU, nephelometric turbidity unit; DTW, depth to water; ft, foot; bls, below land surface; NAVD 88, North American Vertical Datum of 1988; N/A, not applicable; --, not recorded]

Water	Date collected	Air pressure (mmHg)	Air temp (°C)	Water temp (°C)	Dissolved O_2 (mg/L)	pH	Specific conductance (µS/cm)	Alkalinity (mg/L)	Turbidity (NTU)	DTW (ft bls)	Water-level elevation (ft NAVD 88)
Rio Grande at Otowi Bridge (08313000)	August 13, 2009	627	29	19.5	7.5	8.1	296	94.1	65	N/A	N/A
Shallow groundwater wells											
MW-4	December 10, 2014	616.4	12	13.9	7.13	7.79	374	132.4	1.44	52.93	5,954.00
MW-3	December 10, 2014	616.4	12	15.6	4.21	7.69	474	155.7	8.84	108.89	5,850.10
Windmill Well	December 11, 2014	616.9	9	13.4	6.6	7.65	500	143.3	37.6	74.96	5,833.21
Deep groundwater wells											
Industrial Park Well 1	November 6, 2014	627	--	22.3	1.2	8.64	960	375.5	--	153.98	5,700.02
Pow-Wow Well	January 13, 2015	618	-2	15.5	1.6	9.69	357	116	1.5	123.65	5,758.13

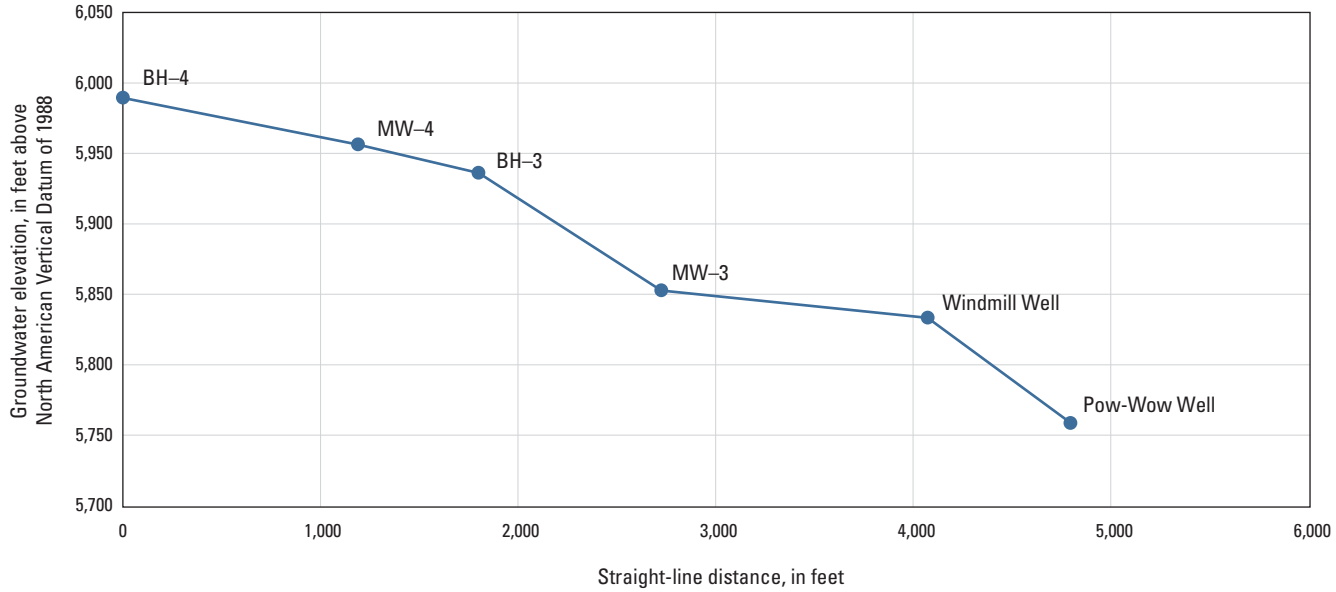

Figure 7. Static water levels in Aquifer Storage and Recovery (ASR)-East measured in November and December 2014, near Pojoaque, New Mexico.

Specific Conductance Profiles

The local recharge inferred from the groundwater elevations would likely require groundwater recharge from precipitation or runoff. One method for determining groundwater recharge from the land surface is the chloride mass balance (CMB) approach (Allison and others, 1994; Murphy and others, 1996). In this study, SC was used as a qualitative proxy for the quantitative recharge determination made with the CMB approach. According to the theory of the CMB approach, atmospheric constituents are deposited on the land surface and infiltrate into the soil. If ET is a larger component of the water budget than infiltration, as is the case of arid and semiarid climates, these constituents accumulate in the root zone as the infiltrating water is removed by transpiring plants (Allison and others, 1994; Phillips, 1994). When plotting the constituent concentrations with depth, the larger concentrations around the root zone appear as a "bulge." By using both a chloride deposition rate and a precipitation rate, the CMB technique allows for the calculation of recharge and the time since recharge, given appropriate assumptions, as outlined by Wood (1999). The use of SC does not allow for such calculations but does provide an indication of whether precipitation is reaching the groundwater or being lost to ET. The SC measured on slurries prepared from the four borings are displayed in figure 8.

Of the four boreholes, only MW–4 displays a large increase in the SC at a specific depth (fig. 8). The "bulge" in SC values in the MW–4 core samples between 15 and 25 ft bls is a strong indication that atmospheric constituents are being evapoconcentrated at the root zone of the native plants and that recharge is unlikely to occur at this site. It is also worth noting that the presence of the highest SC values in the bedrock indicates that rain (or overland surface flow) is able to infiltrate at least partially into the bedrock at this location. The SC throughout the depth profiles of BH–4, MW–3, and BH–3 appears to be relatively constant and far lower, compared with MW–4 (fig. 8). The lack of the characteristic "bulge" in these three other profiles indicates that evapoconcentration of atmospheric constituents in the vadose zone is minimal and that groundwater recharge from precipitation or surface water may occur at these sites. Dissolved constituents in infiltrating water at these locations remain in solution with the wetting front until leaving the vadose zone.

The presence of the "bulge" in the MW–4 depth profile helps to confirm the use of SC slurries on depth profile samples as a screening tool for a more detailed CMB analysis. The SC in the depth profiles of BH-4, MW-3 and BH-3 support the interpretation of groundwater elevations that local recharge of the groundwater by surface processes is possible.

Stable Isotopes of Water

To further evaluate the potential sources of groundwater, ratios of the stable isotopes of water from various sources were compiled and compared. The isotopic compositions (δD and δ^{18}O) of possible end-members (sources) and of the groundwater samples collected from the site were analyzed to spatially and temporally constrain likely sources of groundwater recharge. The variation in the isotopic composition of various potential recharge waters may help identify the source of recharge because of the mass-dependent fractionation of water isotopes (hydrogen and oxygen) resulting from temperature changes during the formation of precipitation and during evaporation prior to infiltration into the aquifer (Genereux and Hooper, 1998; Ingraham, 1998). This mass-dependent fractionation results because the various isotopic forms of water have different vapor pressures. Therefore warmer temperature precipitation contains a greater number of heavier isotopes (less negative δ^{18}O and δD values) than cooler temperature precipitation (Ingraham, 1998). Similarly, the water left after evaporation will contain a larger number of heavier isotopes than water that has not been subjected to evaporation.

The stable-isotope ratios of water from groundwater samples collected from wells in the study area, surface water from the Rio Grande and San Juan River, and groundwater from deep wells in the San Juan Basin are plotted in figure 9. The stable-isotope ratios are reported table 8.

The δ^{18}O and δD values of the groundwater samples collected in the study area plot below and to the right of the Global Meteoric Water Line (GMWL) (Craig, 1961) and a local meteoritic line developed from average precipitation above Santa Fe, N. Mex., by Anderholm (1994) (fig. 9). The overall position of the δD and δ^{18}O values for wells in this study compared to the GMWL is typical of the arid and semiarid climate of the southwestern United States, where there is a large evaporation component to the water budget (Friedman and others, 1992). The groundwater samples do plot close to the meteoric line for the Upper Colorado River watershed (Kendall and Coplen, 2001) (fig. 9). The Upper Colorado River meteoric line is an unweighted linear regression generated from 214 analyses of stream samples collected from 19 selected sites within the USGS National Stream Quality Accounting Network and Hydrologic Benchmark Network. For comparison, the average δ^{18}O and δD values of four samples collected from the San Juan River near Shiprock, N. Mex. (approximately 170 miles northwest of the site), between the fall of 2010 and spring of 2012 (Robertson and others, 2016; fig. 9) and the average of 101 samples collected from the Rio Grande in Albuquerque, N. Mex. (approximately 65 miles southwest of the site) (Plummer and others, 2012; fig. 9) essentially plot directly on the meteoric line for the Upper Colorado River watershed. Like many rivers in the Upper Colorado River watershed, the San Juan River and the Rio Grande are primarily sourced by high-elevation snowpack and precipitation and thus would be expected to have a lighter isotopic composition than the lower elevation local precipitation.

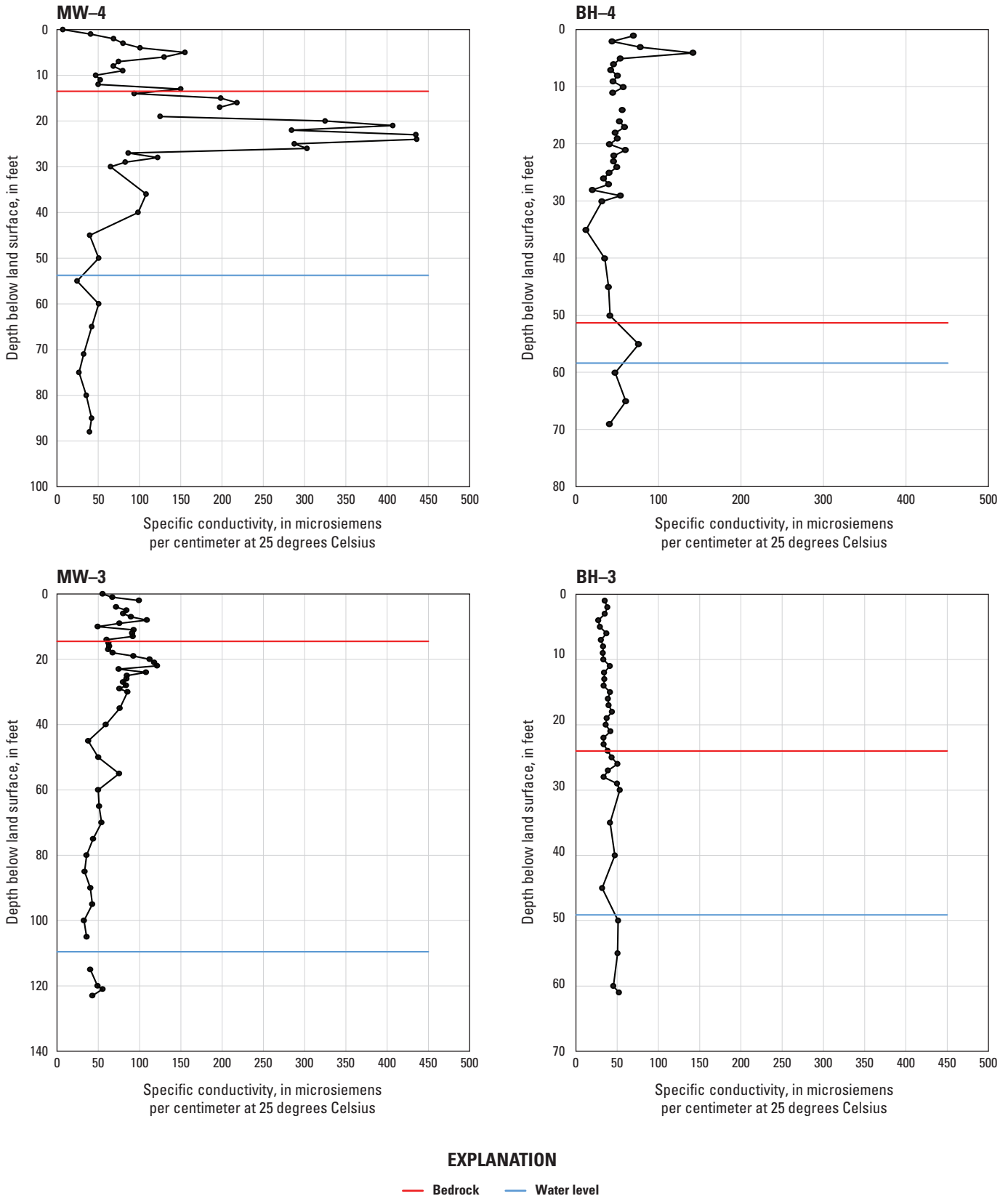

Figure 8. Specific conductance profiles of slurries prepared from core samples, Pojoaque, New Mexico.

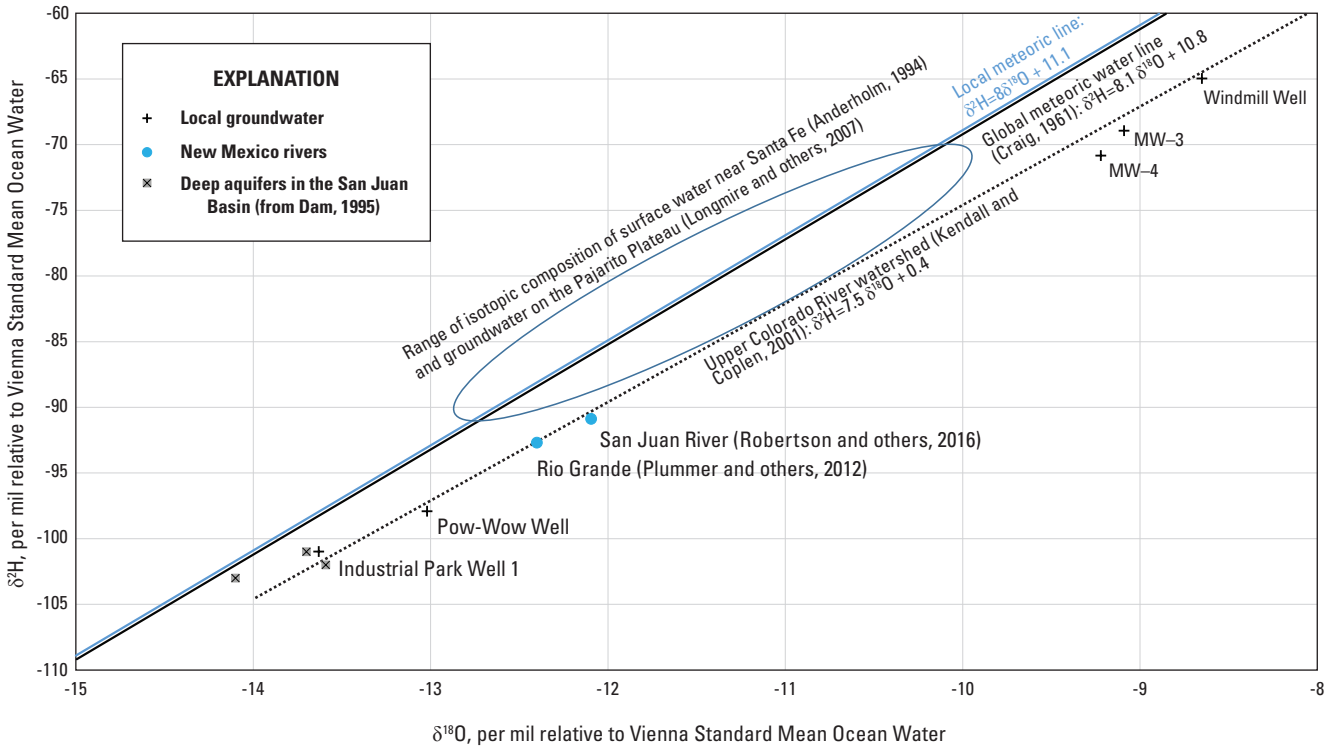

Figure 9. The delta deuterium (δD) and delta oxygen-18 ($\delta^{18}O$) compositions of groundwater samples collected from wells in the study area, surface water from the Rio Grande and San Juan River, and groundwater from deep wells in the San Juan Basin, New Mexico.

Table 8. Isotopic values of groundwater samples collected from wells, Pojoaque, New Mexico.

[pCi/L, picocurie per liter; TU, tritium unit; δD, isotopic composition of deuterium in per mil relative to Vienna Standard Mean Ocean Water; ‰, per mil; $\delta^{18}O$, isotopic composition of oxygen-18 in per mil relative to Vienna Standard Mean Ocean Water; $\delta^{13}C$, isotopic composition of carbon-13 in per mil relative to Vienna Pee Dee Belemnite; ^{14}C, carbon-14 activity in percent modern carbon (pmC)]

Site name	Date collected (mm–dd–yyyy)	Tritium		δD (‰)	$\delta^{18}O$ (‰)	$\delta^{13}C$ (‰)	^{14}C (pmC)
		(pCi/L)	(TU)				
Shallow groundwater wells							
MW-4	12–10–2014	0.30	0.09	-70.9	-9.22	-8.98	34.6%
MW-3	12–10–2014	0.60	0.19	-69.00	-9.09	-10.91	49.4%
MW-3 Replicate	12–10–2014	-0.03	-0.01	-69.7	-9.15	-11.04	49.2%
Windmill Well	12–11–2014	0.02	0.01	-65.0	-8.65	-8.02	77.5%
Deep groundwater wells							
Pow-Wow Well	1–13–2015	0.20	0.06	-97.9	-13.02	-9.66	17.8%
Industrial Park Well 1	11–6–2014	0.21	0.07	-101.4	-13.63	-4.75	0.6%

The large difference in the stable-isotope ratios provides evidence that the shallow groundwater wells (MW–3, MW–4, and the Windmill Well) are hydrologically distinct from the deeper wells (Pow-Wow Well and Industrial Park Well 1) (fig. 9). The relatively enriched $\delta^{18}O$ and δD values of the shallow groundwater wells compared with the deeper wells suggests a warmer, lower-elevation source for the recharge, such as local precipitation. The range of the $\delta^{18}O$ and δD values in the shallow wells may result from seasonal influences on the stable-isotopic composition of precipitation. Seasonal variations in the isotopic composition of local precipitation are caused by the differences in the temperature of condensation of atmospheric water vapor or from the source of the precipitation (Ingraham, 1998). Storms moving into the area primarily from the Pacific Ocean during the winter would have lighter compositions than thunderstorms originating primarily in the Gulf of Mexico or in the southern Pacific Ocean during the summer (Ingraham, 1998).

The composition of δD and $\delta^{18}O$ in the groundwater sample from Industrial Park Well 1 is similar to the composition of stable isotopes compiled for groundwater samples from the deeper aquifer units underlying the Mancos Shale as part of the San Juan Basin Regional Aquifer-System Analysis study conducted by the USGS (Dam, 1995). On the basis of the work by Phillips and others (1986), Dam (1995) concluded that these stable-isotope compositions represented groundwater that recharged during the Pleistocene Epoch. Lower mean annual temperatures during the Pleistocene Epoch likely resulted in lighter isotopic ratios of precipitation entering the groundwater (Phillips and others, 1986).

It is evident that the shallow groundwater in the study area has a stable-isotope composition substantially more enriched in the heavier isotopes of oxygen and hydrogen than that of the deeper groundwater in the study area (fig. 9, table 8). This difference in the compositions strongly supports a local recharge mechanism from the surface for the shallow groundwater and an older (and [or] higher elevation) recharge source for the deeper groundwater.

Age-Dating Constituents

Age-dating constituents, measured in groundwater samples, are evaluated to provide additional evidence for current recharge mechanisms. The groundwater ages indicated by ^{3}H and radiocarbon concentrations help to constrain the conceptual model of recharge.

Tritium

One advantage to using ^{3}H as an age indicator is that it is incorporated into the water molecule and is not affected by chemical reactions, microbial degradation, or other reactions that complicate the interpretation of other tracers (Clark and Fritz, 1997). The ^{3}H measured in all groundwater samples was below 0.2 TU (table 8). On the basis of these results, all of the groundwater samples are considered to represent groundwater that recharged before the year 1950. Because of the previous evidence supporting local recharge in the shallow wells, one might expect the water in the shallow groundwater to be younger; however, descriptions of the heterogeneous bedrock lithology suggest that impermeable layers and disconnected flow paths may limit the groundwater recharge of infiltrating waters. The local recharge to the Tesuque Formation is therefore thought to occur only where the more permeable layers outcrop on the surface or subcrop beneath the channel sands. Once recharged, the shallow groundwater moves at low velocities and its flow is restricted by the interbedded clays. Although other evidence suggests surface processes as a recharge mechanism, the ^{3}H results demonstrate that the recharge is limited and that managed recharge to the bedrock may be unfavorable at these locations.

Radiocarbon

The ^{14}C concentrations reported for the shallow wells, MW–3, MW–4, and Windmill Well, were 49 pmC, 35 pmC, and 78 pmC, respectively. In comparison, the ^{14}C concentrations reported for the deep wells, Industrial Park Well 1 and Pow-Wow Well, were less than 1 pmC and 18 pmC, respectively (table 8). Assuming that the initial ^{14}C content at the time of recharge (A_0) is 100 pmC (equation 2), the unadjusted radiocarbon ages of the shallow groundwater samples are between 2,000 and 8,800 years, which is consistent with the ^{3}H results. The radiocarbon ages of the samples from the Pow-Wow Well and Industrial Park Well 1 were calculated to be 14,200 years and 41,700 years, respectively.

The accuracy of the radiocarbon age is dependent upon the value estimated for A_0; therefore, understanding the possible contributions to higher or lower A_0 values is important for constraining the radiocarbon age. Until the nuclear weapons testing in the 1950s and 1960s, the activity of ^{14}C in the DIC of atmospheric moisture had been fairly constant at 100 pmC (Wang and others, 1998). The nuclear weapons tests added substantial quantities of ^{14}C into the atmosphere, which resulted in $^{14}CO_2$ in groundwater above 100 pmC. Because of the low ^{3}H results reported in the groundwater at the site, none of the groundwater samples are considered to have initial ^{14}C activities that were above 100 pmC because of the nuclear tests. Upon reaching the land surface, reactions between atmospheric DIC and soil carbonates and silicate minerals can result in A_0 values substantially different (usually lower) than 100 pmC. Other processes that may contribute lower inorganic ^{14}C activity to the groundwater include carbonate mineral dissolution, coalification, methane production, metamorphism of carbonate rocks, and anaerobic biochemical decomposition of organic material (Wigley and others, 1978; Phillips and others, 1986). The effect of these processes on the dissolved radiocarbon content of the groundwater is known as fossil carbon dilution. The smaller ^{14}C concentration in the groundwater DIC that results from these processes would result in smaller ^{14}C

concentrations measured at the time the sample was collected. The radiocarbon age of the sample would be estimated to be older than the actual age if A_0 was assumed to be 100 pmC in equation 2.

Because the radiocarbon age was estimated by using 100 pmC for A_0 in this investigation, it is likely that the estimated radiocarbon ages are older than the actual ages; however, the radiocarbon age differences between the samples of the shallow and the deeper groundwater are large enough to support evidence presented earlier in this report that the shallow groundwater is recharged locally and is not a large component of the deeper regional system.

Geochemical Suitability of the Study Area for Managed Recharge Waters

Groundwater in the Tesuque Formation is generally reported to be hard to very hard, indicating high concentrations of calcium bicarbonate (Ca-HCO_3) (Arctic Slope Consulting Group and John Shomaker and Associates, Inc., 2003). Locally, water in the Tesuque Formation is also reported to have concentrations of U, As, and (or) F above the corresponding EPA MCLs. An assessment of the groundwater geochemistry at the Pueblo of Pojoaque, N. Mex., indicates that wells in the study area that produce water from shallow depths (<200 ft deep) produce high concentrations of U relative to drinking water standards (McQuillan and Montes, 1998).

Subsurface Mineralogy and Elemental Chemistry

The clay content by weight of samples collected in the unconsolidated deposits above the bedrock was generally lower than that of samples collected from the bedrock (table 4). Quartz was the most prominent mineral in all but three samples, each of which had a clay content above 40 percent. The high quartz and aluminosilicate mineral composition of the unconsolidated deposits and the underlying bedrock, relative to more soluble evaporite content, indicate that the solid phases have undergone dissolution since deposition. Based on the hydrogeologic evidence presented earlier in this report of local recharge, the mineral composition is likely the result of weathering from atmospheric waters that dissolved and displaced the more soluble minerals.

Arsenic and U are redox-sensitive elements that tend to be more soluble in oxidizing water (Hem, 1985; Manning and Goldberg, 1997); therefore, as the solid phases are exposed to more oxidative weathering, these constituents would leach out. If the oxic weathering were to occur for long periods, one would expect reduced concentrations in the groundwater in contact with weathered deposits relative to equivalent unweathered deposits. This conceptual weathering model would be expected in fluvial deposits and in the shallow bedrock underlying them, similar to the lithologies described in this investigation. The presence of clay layers, however, could slow groundwater velocities and allow for concentrations of constituents to be locally higher. Because of the lower permeabilities, the presence of these clay and fine-grained deposits may retard the weathering process.

Results of the whole-rock and anion analyses are found in table 9. All the samples collected from the cores had detectable U (1.0 to 37 milligrams per kilogram-dry [mg/kg-dry]); however, all the core samples had concentrations of constituents of concern below the New Mexico residential soil screening criteria, with the exception of one sample with a high clay content. This sample had an As concentration (4.7 mg/kg-dry) that exceeded the screening criteria for As (4.25 mg/kg) (New Mexico Environment Department, 2015). Based on the mineralogy and chemical analysis of the solid phase samples, the constituents of concern are not likely to be leached out in quantities that would result in groundwater concentrations that exceed regulatory limits.

Table 9. Cation and anion concentrations in selected borehole samples from near Pojoaque, New Mexico.

[Values exceeding NMED Residential Soil Screening Levels (New Mexico Environment Department, 2015) are shown in RED. mg/kg-dry, milligram per kilogram on a dry weight basis; EPA, U.S. Environmental Protection Agency; ft, foot; bls, below land surface; NMED SSL, New Mexico Environment Department Soil Screening Levels; N/A, not applicable; <, less than; %, weight percent]

Site designation	Whole rock metal analysis (mg/kg-dry) by EPA's Method SW846 6020A									
	Depth (ft bls)	Aluminum	Antimony	Arsenic	Barium	Beryllium	Cadmium	Calcium	Chromium	Cobalt
BH-4	19–20	1,800	0.04	0.71	27.0	0.25	0.07	3,200	1.7	1.2
BH-4	28–29	15,000	0.22	4.70	360.0	1.20	0.34	18,000	14.0	6.8
BH-4	30–31	2,000	0.08	3.10	45.0	0.30	0.08	4,700	3.1	1.9
BH-4	50–51	4,600	0.05	2.60	820.0	0.39	0.13	15,000	4.0	2.9
BH-4	56–57	2,600	<0.19	1.20	71.0	0.23	0.19	80,000	3.3	1.8
MW-4	12–13	2,700	<0.19	0.97	50.0	0.26	0.13	15,000	3.4	1.7
MW-4	36–37	9,300	0.10	1.60	300.0	0.48	0.25	11,000	6.6	4.5
MW-4	54–55	9,200	0.12	1.80	77.0	0.68	0.30	6,000	5.0	3.9
MW-4	74–75	11,000	0.20	2.40	150.0	0.93	0.61	13,000	7.3	5.3
MW-4	86–87	7,900	0.13	1.40	160.0	0.45	0.21	6,600	5.5	3.8
BH-3	10–11	2,100	0.06	0.86	57.0	0.28	0.12	9,700	2.8	1.4
BH-3	20–21	2,500	0.05	0.94	82.0	0.32	0.10	8,300	3.3	1.6
BH-3	24–25	7,100	0.12	1.70	130.0	0.49	0.23	18,000	5.9	3.5
BH-3	46–47	2,600	0.04	0.81	26.0	0.25	0.10	7,000	2.9	1.3
BH-3	60–61	26,000	0.24	3.20	97.0	1.20	0.50	47,000	18.0	9.3
MW-3	13–14	4,900	0.11	1.30	180.0	0.58	0.27	22,000	6.1	3.0
MW-3	42–43	19,000	0.25	1.90	100.0	1.10	0.78	97,000	12.0	7.6
MW-3	93–94	6,800	0.16	1.10	54.0	0.53	0.18	15,000	11.0	4.0
MW-3	114–115	8,000	0.15	0.89	810.0	0.41	0.18	15,000	8.4	3.0
MW-3	123–124	15,000	0.29	1.00	180.0	0.73	0.33	19,000	16.0	7.5
	NMED SSL	78,002	31.29	4.25	15,600	156	70.5	N/A	96.6*	N/A

Site designation	Whole rock metal analysis (mg/kg-dry) by EPA's Method SW846 6020A										
	Depth (ft bls)	Copper	Iron	Lead	Magnesium	Manganese	Molybdenum	Nickel	Potassium	Selenium	Silicon
BH-4	19–20	2.1	2,900	1.8	770	70	<0.70	2.1	420	0.28	410
BH-4	28–29	12.0	15,000	11.0	5,400	150	<0.90	13.0	3,400	0.49	290
BH-4	30–31	2.2	4,900	2.0	880	54	<0.76	2.7	530	0.42	530
BH-4	50–51	4.0	5,900	2.8	1,600	130	<0.70	8.1	990	0.24	390
BH-4	56–57	2.5	4,100	1.7	1,200	82	<0.72	4.8	670	<0.72	370
MW-4	12–13	3.1	4,700	2.5	1,300	100	<0.79	3.4	730	0.30	530
MW-4	36–37	6.5	10,000	4.8	3,200	150	<0.86	8.2	2,600	<0.86	420
MW-4	54–55	5.2	9,200	6.3	3,600	210	<0.91	8.1	2,100	<0.91	350
MW-4	74–75	8.6	12,000	8.9	5,300	260	<0.80	11.0	3,400	<0.80	250
MW-4	86–87	5.5	10,000	4.2	2,600	200	<0.80	6.7	2,000	0.24	340
BH-3	10–11	2.7	3,700	2.1	1,100	67	<0.85	2.9	540	<0.85	530
BH-3	20–21	2.6	5,900	2.7	1,100	98	<0.82	3.0	550	<0.82	500
BH-3	24–25	5.3	8,700	4.8	3,000	160	<0.80	6.8	1,800	<0.80	430
BH-3	46–47	2.1	4,800	2.2	1,100	75	<0.72	2.9	630	<0.72	330
BH-3	60–61	26.0	25,000	12.0	9,800	400	<0.84	20.0	6,200	0.49	500
MW-3	13–14	6.0	6,300	4.6	2,800	180	<0.74	6.1	1,800	0.24	570
MW-3	42–43	20.0	19,000	11.0	9,900	940	<0.87	16.0	8,000	0.60	530
MW-3	93–94	8.7	9,600	4.9	3,700	210	<0.82	8.5	1,700	<0.82	450
MW-3	114–115	5.6	9,000	3.7	2,600	190	<0.74	6.3	1,600	<0.74	380
MW-3	123–124	10.0	19,000	7.8	6,700	350	<0.87	17.0	3,100	0.32	430
	NMED SSL	3,130	54,800	400	N/A	10,550	391	1,560	N/A	391	N/A

Table 9. Cation and anion concentrations in selected borehole samples from near Pojoaque, New Mexico.—Continued

[Values exceeding NMED Residential Soil Screening Levels (New Mexico Environment Department, 2015) are shown in RED. mg/kg-dry, milligram per kilogram on a dry weight basis; EPA, U.S. Environmental Protection Agency; ft, foot; bls, below land surface; NMED SSL, New Mexico Environment Department Soil Screening Levels; N/A, not applicable; <, less than; %, weight percent]

Site designation	Whole rock metal analysis (mg/kg-dry) by EPA's Method SW846 6020A					Inorganic Anions (mg/kg-dry) by EPA's Method SW9056					Moisture content (%)
	Depth (ft bls)	Silver	Sodium	Uranium	Zinc	Bromide	Chloride	Fluoride	Nitrate	Sulfate	
BH-4	19–20	0.02	28	1.0	6.8	<1.40	1.4	2.1	0.26	3.1	<1.0
BH-4	28–29	0.09	73	6.9	44.0	<1.70	1.5	8.2	0.39	8.4	19.0
BH-4	30–31	0.04	25	2.6	8.0	<1.40	1.2	2.5	0.31	4.0	3.1
BH-4	50–51	0.03	49	3.1	12.0	<1.60	1.3	9.5	0.49	85.0	8.2
BH-4	56–57	<0.12	45	1.8	9.3	<1.40	17.0	2.2	0.29	11.0	2.5
MW-4	12–13	<0.12	110	2.3	10.0	<1.40	1.4	1.9	0.64	6.2	<1.0
MW-4	36–37	0.04	360	4.9	24.0	<1.50	22.0	3.5	1.70	73.0	10.0
MW-4	54–55	0.09	330	5.1	23.0	<1.60	2.8	15.0	1.00	8.5	14.0
MW-4	74–75	0.21	160	5.8	43.0	<1.60	2.7	7.7	0.44	7.3	15.0
MW-4	86–87	0.07	110	4.2	23.0	<1.60	3.9	3.0	0.41	8.4	15.0
BH-3	10–11	0.02	36	1.9	8.4	<1.40	1.3	2.2	0.25	4.3	3.3
BH-3	20–21	0.03	34	1.8	8.9	<1.40	1.7	1.4	0.26	5.4	3.2
BH-3	24–25	0.06	47	3.2	22.0	<1.50	2.7	6.3	0.62	2.8	8.3
BH-3	46–47	0.02	28	1.6	9.2	<1.50	1.1	1.9	0.29	6.0	6.9
BH-3	60–61	0.12	210	9.3	64.0	<1.80	3.7	8.8	0.92	14.0	21.0
MW-3	13–14	0.07	140	7.1	20.0	<1.40	6.7	6.8	0.85	24.0	2.7
MW-3	42–43	0.19	390	37.0	54.0	<1.60	14.0	8.1	1.10	37.0	15.0
MW-3	93–94	0.07	95	5.0	27.0	<1.70	3.9	2.8	0.50	9.5	18.0
MW-3	114–115	0.04	150	5.2	21.0	<1.60	3.0	1.5	0.45	9.0	14.0
MW-3	123–124	0.11	150	9.5	44.0	<1.70	4.1	3.7	0.49	14.0	22.0
	NMED SSL	391	N/A	234	23,464	N/A	N/A	4,693	125,000	N/A	N/A

*Chromium exceedance values based on total.

Major Ions and Trace Metals

The complete set of groundwater analytical data collected during this study is available in table 10. The piper diagram is a trilinear diagram useful for illustrating the hydrochemical facies of a water sample (Hem, 1985). The percentages on the axes of the diagram represent the relative abundance of ions in percent milliequivalents. Examination of the major ions (fig. 10) illustrates the different hydrochemical facies between the shallow wells (MW–3, MW–4, and the Windmill Well) and the deep wells (Pow-Wow Well and Industrial Park Well 1).

Cations are dominated by Ca in the shallower wells and by Na in the deeper wells. Given the similar anion compositions in the two sets of groundwater samples and the observed and reported presence of clay, cation exchange may be responsible for the distinct facies. McQuillan and Montes (1998) also reached this conclusion and attributed the change in cation concentrations at depth to the evolution of groundwater through cation exchange, resulting in a change from a Ca-HCO_3 to a Na-HCO_3 or Na-SO_4 hydrochemical facies. An increase in pH and F concentrations was also associated with this evolution (McQuillan and Montes, 1998). The field parameters collected during this investigation similarly showed an increase in pH between the shallower wells and the deeper wells. Table 7 shows that the pH for deeper wells is above 8 and the pH for the shallower wells is below 8. The pH of groundwater tends to increase with residence time because water-rock interactions typically consumes hydrogen ions (Stumm and Morgan, 1996). One additional parameter of note is the dissolved oxygen, which is much lower in the deep wells (<2 mg/L) relative to the shallow wells (>4 mg/L), supporting the groundwater elevation and isotopic evidence that the groundwater in the shallow wells is recharged locally and that the groundwater in the deeper wells represents a longer flow path.

Table 10. Dissolved metals and anions in groundwater samples from near Pojoaque, New Mexico.

[EPA Drinking Water Standard Exceedances (U.S. Environmental Protection Agency, 2009) are shown in RED. mm, month; dd, day; yyyy, year; mg/L, milligram per liter; <, less than; EPA, U.S. Environmental Protection Agency; --, no standard reported; TDS, total dissolved solids]

Site designation	Date collected (mm–dd–yyyy)	Dissolved metals by inductively coupled plasma (mg/L)								
		Aluminum	Antimony	Arsenic	Barium	Beryllium	Boron	Cadmium	Calcium	Chromium
MW-4	12–10–2014	0.007	0.00008	0.003	0.025	<0.00002	0.0550	<0.00003	41.60	0.0034
MW-3	12–10–2014	0.007	0.00008	0.003	0.061	<0.00002	0.0529	0.00004	49.79	0.0020
MW-3 Replicate	12–10–2014	0.007	0.00007	0.003	0.062	<0.00002	0.0522	0.00004	49.33	0.0020
Windmill Well	12–11–2014	<0.003	0.00006	0.001	0.086	<0.00002	0.0592	0.00012	60.35	<0.0003
Pow-Wow Well	1–13–2015	0.015	0.00007	0.010	0.002	<0.00002	0.1763	<0.00003	3.58	0.0017
Industrial Park Well 1	11–6–2014	0.010	<0.000027	0.028	0.003	0.00004	0.4784	<0.00003	2.35	<0.0003
EPA drinking water standards		0.05 to 0.2*	0.006	0.010	2	0.004	--	0.005	--	0.1

Site designation	Date collected (mm–dd–yyyy)	Dissolved metals by inductively coupled plasma (mg/L)								
		Cobalt	Copper	Iron	Lead	Lithium	Magnesium	Manganese	Molybdenum	Nickel
MW-4	12–10–2014	0.0001	<0.0008	<0.004	0.0002	0.031	3.904	0.005	0.002	0.001
MW-3	12–10–2014	0.0022	<0.0008	0.004	0.0002	0.048	4.642	0.006	0.003	0.001
MW-3 Replicate	12–10–2014	0.0021	<0.0008	0.009	0.0002	0.047	4.691	0.005	0.003	0.001
Windmill Well	12–11–2014	0.0003	0.001	0.027	0.0002	0.051	5.574	0.041	0.004	0.001
Pow-Wow Well	1–13–2015	<0.00005	<0.0008	0.012	0.0015	0.087	0.033	<0.40	0.003	0.000
Industrial Park Well 1	11–6–2014	<0.00005	0.004	0.049	0.0006	0.205	0.067	0.007	0.019	<0.0002
EPA drinking water standards		--	1.3	0.3*	0.015	--	--	0.05*	--	--

Site designation	Date collected (mm–dd–yyyy)	Dissolved metals by inductively coupled plasma (mg/L)								
		Potassium	Selenium	Silver	Sodium	Strontium	Titanium	Uranium	Vanadium	Zinc
MW-4	12–10–2014	3.7610	0.002	<0.00002	28.38	0.5814	<0.00003	0.010	0.0071	0.0085
MW-3	12–10–2014	3.915	0.004	<0.00002	39.03	0.7402	<0.00003	0.023	0.0088	0.0426
MW-3 Replicate	12–10–2014	3.7570	0.004	<0.00002	36.56	0.7477	<0.00003	0.023	0.0089	0.0413
Windmill Well	12–11–2014	2.9340	0.004	<0.00002	39.00	0.8366	<0.00003	0.018	0.0041	0.1346
Pow-Wow Well	1–13–2015	0.6350	0.003	<0.00002	80.70	0.0372	<0.00003	0.024	0.0041	0.0085
Industrial Park Well 1	11–6–2014	1.629	<0.00005	<0.00002	225.80	0.0203	<0.00003	0.000	<0.0001	<0.002
EPA drinking water standards		--	0.05	0.10*	--	--	0.002	0.03	--	5*

Table 10. Dissolved metals and anions in groundwater samples from near Pojoaque, New Mexico.—Continued

[EPA Drinking Water Standard Exceedances (U.S. Environmental Protection Agency, 2009) are shown in RED. mm, month; dd, day; yyyy, year; mg/L, milligram per liter; <, less than; EPA, U.S. Environmental Protection Agency; --, no standard reported; TDS, total dissolved solids]

Site designation	Date collected (mm–dd–yyyy)	Dissolved anions by ion chromatography							
		Bromide	Chloride	Fluoride	Nitrite (as N)	Nitrate (as N)	Sulfate	Silica	TDS
MW-4	12–10–2014	0.250	13.78	0.439	0.002	1.471	32.26	26.1100	256.84
MW-3	12–10–2014	0.294	18.83	0.607	0.013	0.877	49.88	26.92	292.82
MW-3 Replicate	12–10–2014	0.297	19.00	0.600	0.013	0.788	51.83	26.8900	322.04
Windmill Well	12–11–2014	0.199	15.26	0.991	0.005	3.590	66.51	22.4100	321.10
Pow-Wow Well	1–13–2015	0.158	11.25	1.301	0.001	0.993	42.79	19.7800	234.49
Industrial Park Well 1	11–6–2014	0.157	10.40	6.214	<0.001	<0.04	44.07	17.5800	581.88
EPA drinking water standards		--	250*	4.0	1	10.0	250*	--	500*

*EPA Secondary Drinking Water Standards.

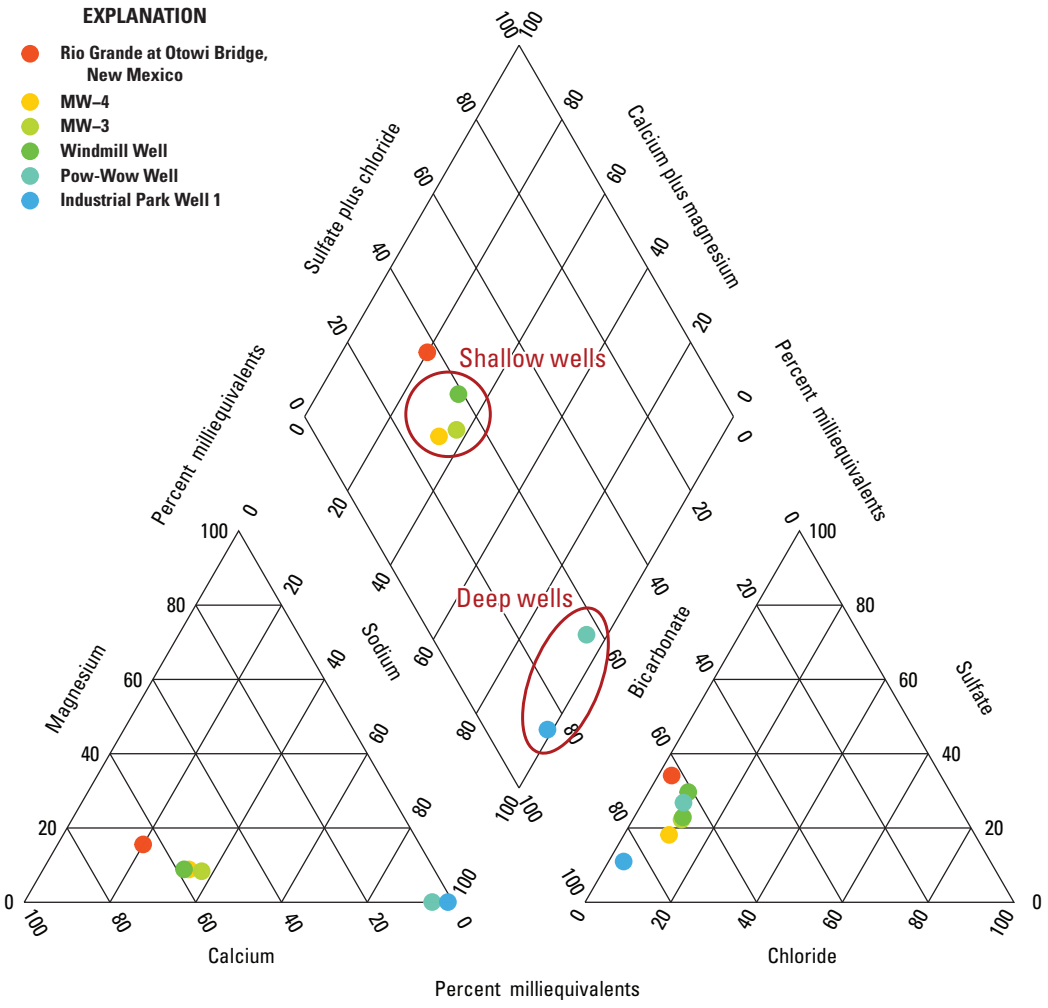

Figure 10. Major-ion relations in the groundwater during winter 2014 and 2015 for the study area near Pojoaque, New Mexico.

The constituents of concern in the Tesuque Formation are As, F, and U and are likely due to deposits from Tertiary volcanism (McQuillan and Montes, 1998; McLemore and others, 2011). Only the sample from the deep Industrial Park Well 1 exceeded any State or Federal drinking-water standards. Arsenic (0.028 mg/L) and F (6.2 mg/L) exceeded their corresponding health-based EPA MCLs, and the DS concentration (582 mg/L) exceeded the Secondary Maximum Contaminant Level for total DS, which is based on aesthetic considerations (table 10; U.S. Environmental Protection Agency, 2009). The composition of the shallow, native groundwater suggests that storing water diverted from the Rio Grande is not likely to lead to exceedances of the health-based EPA MCLs in the stored water.

Evaluating the Favorability of the Site for Managed Aquifer Recharge by Surface Infiltration

The results of this investigation suggest that there are several favorable characteristics of the two arroyos to managed aquifer recharge by surface infiltration, including the fact that the composition of the shallow groundwater and elemental chemistry and mineral make-up of the unconsolidated channel deposits and shallow bedrock suggest that storing water diverted from the Rio Grande is not likely to lead to exceedances of the health-based EPA MCLs in the stored water. However, geochemical modeling would be a useful exercise to verify this finding. The low storage-potential of the channel deposits and shallow bedrock, however, along with the need for significant infrastructure to retain applied water at the site, present challenges.

The channel capacity and infiltration rates measured in the two reaches suggest that water could be applied to the channels at a rate higher than the estimated supply need for 50 percent of the daily water-use requirements reported for the project and lower than the channel capacity for flood flows. However, because there was no saturation observed in the unconsolidated deposits shortly after a large precipitation event, it is thought that water infiltrating into the channels runs out of the reaches quickly by flowing along the top of the bedrock. An engineering solution such as a subsurface dam would be required to limit the losses out of the reach from subsurface flow through the unconsolidated deposits.

The results of this investigation also demonstrate that shallow groundwater is likely recharged by local precipitation, and therefore indicate that there is the potential for recharge by surface infiltration. The concentrations of age-dating tracers measured in the groundwater, however, suggest that the recharge is low and may be limited by the fine-grained lithology that was observed in the subsurface cores. The fine-grained lithology of the shallow bedrock also suggests limited storage as evidenced by the artesian conditions observed. The limited recharge and storage capacity in the two reaches limits the potential for managed aquifer recharge by surface infiltration.

Summary

In order to provide long-term storage of diverted surface water from the Rio Grande as part of the Aamodt water rights settlement, managed aquifer recharge by surface infiltration in Pojoaque River Basin arroyos was proposed as an option. The initial hydrogeologic and geochemical characterization of two arroyos located within the Pojoaque River Basin was performed in 2014 and 2015 in cooperation with the Bureau of Reclamation to evaluate the potential suitability of these two arroyos as sites for managed aquifer recharge through surface infiltration. The selected stream reaches were high gradient, with an average slope of 3.0 percent in ASR-East and 3.5 percent in ASR-West; the maximum slopes were 10.0 percent and 9.2 percent, respectively. The channels in both arroyos are braided, and the thalweg and bankfull heights are irregular, making water-surface profile computations for selected discharges difficult and making the channels unsuitable for streamgaging. The calculated discharges that would result in overbank flows are greater than 2,000 cubic feet per second (ft^3/s) and greatly exceed those potentially to be used for managed recharge, indicating that the channel capacity is favorable for managed recharge.

The geophysical resistivity surveys conducted as part of this investigation were effective at imaging the contact between the coarse sands (resistivity above 70 ohmmeters) of the arroyo channel and the siltier sands and clays of the bedrock (resistivity below 20 ohmmeters) in the adjacent hills and below the channel. The bedrock, however, was too conductive to effectively image any subtle structures, such as preferential groundwater pathways, or the water table. The resistivity surveys showed that the sand and gravel channel was generally 30–50 feet thick. Assuming a porosity of 40 percent for the channel sands, there is probably less than 300 acre-feet of storage potential in the channel sands of the two reaches.

On the basis of the observations made during drilling and the descriptions of the cores, the coarse-grained deposits of the channel sands appeared to be very permeable and well connected despite the occasional fine-grained clay lenses. The semiconfined conditions observed in the bedrock borings and the presence of expanding clays suggest limited effective storage in the bedrock. The lithology of the channel sands is favorable to managed recharge, but the small volume places limits on water-storage potential. Although groundwater was found in the bedrock, the prevalence of the fine-grained deposits limits the effective storage of applied water and suggests that recharge of more permeable layers may only occur on the outcrops or where those layers subcrop in the channel bottom.

Infiltration rates measured on a variety of channel morphologies in the study reaches were extremely large (9.7–94.5 feet per day), indicating that the channels could potentially accommodate as much as 6.6 cubic feet per second of applied water without generating surface runoff out of the reach; however, the small volume of storage in the unconsolidated channel sands and the potential for the majority of water to flow over the bedrock contact out of the reach present a challenge for storing water.

Saturation was not observed in the unconsolidated channel sands in four subsurface borings but was found at 7–60 feet below the contact between the unconsolidated channel sands and the bedrock. The measured water levels indicate a horizontal groundwater gradient that generally follows the local topography. The vertical groundwater gradient between the shallow wells and those wells screened deeper indicates that recharge to the shallow groundwater is by local precipitation. The ability for local recharge to occur from precipitation is favorable to managed recharge because it indicates an existing pathway for surface water to reach the aquifer units underlying the channel.

Local recharge of the shallow groundwater observed in this investigation was supported by geochemical and isotopic signatures, which also indicated that the deeper groundwater at the site may be associated with longer regional groundwater flow paths. The two age-dating tracers measured in this investigation indicate that the shallow groundwater flow paths are very slow and demonstrate that the local recharge is limited and conditions may be unfavorable to managed recharge.

The channel sands and the shallow bedrock were observed to be weathered in the cores collected from the subsurface, indicating the movement of oxic groundwater following deposition. This observation was supported by the whole-rock elemental analysis and mineralogy of several core samples. Based on the chemical analysis of the selected solid phase samples, the constituents of concern are not likely to be leached in quantities that would result in concentrations that would exceed regulatory limits in the stored water. The presence of clays, however, may cause some local exceedances. The composition of the shallow, native groundwater also suggests that storing water diverted from the Rio Grande is not likely to lead to exceedances of the health-based U.S. Environmental Protection Agency Maximum Contaminant Levels in the stored water.

References Cited

Aldridge, B.N., and Garrett, J.M., 1973, Roughness coefficients for stream channels in Arizona: U.S. Geological Survey Open-File Report, 87 p.

Allison, G., Gee, G.W., and Tyler, S.W., 1994, Vadose-zone techniques for estimating groundwater recharge in arid and semiarid regions: Soil Science Society of America Journal, v. 58, no. 1, p. 6.

American Society for Testing and Materials, 2006, ASTM D2434-68(2006), standard test method for permeability of granular soils (constant head) (withdrawn 2015): ASTM International, West Conshohocken, Pa., www.astm.org.

American Society for Testing and Materials, 2009, ASTM D7263-09, standard test methods for laboratory determination of density (unit weight) of soil specimens: ASTM International, West Conshohocken, Pa., www.astm.org.

American Society for Testing and Materials, 2010, ASTM D2216-10, standard test methods for laboratory determination of water (moisture) content of soil and rock by mass: ASTM International, West Conshohocken, Pa., www.astm.org.

American Society for Testing and Materials, 2016a, ASTM D5084-16a, standard test methods for measurement of hydraulic conductivity of saturated porous materials using a flexible wall permeameter: ASTM International, West Conshohocken, Pa., www.astm.org.

American Society for Testing and Materials, 2016b, ASTM D2216-10, standard test methods for laboratory determination of water (moisture) content of soil and rock by mass: Annual book of ASTM standards, ASTM International, West Conshohocken, Pa., www.astm.org.

Anderholm, Scott K., 1994, Ground-water recharge near Santa Fe, north-central New Mexico: U.S. Geological Survey Water-Resources Investigations Report 94–4078, 68 p.

Arctic Slope Consulting Group and John Shomaker and Associates, Inc., 2003, Aamodt feasibility study, final report for task 3: Deep Well/Well Field Investigation and Integration, accessed March 18, 2015, at http://www.ose.state.nm.us/water-info/AamodtSettlement/appendix18.pdf.

Argonne National Laboratory, 2015, Data collection handbook to support modeling impacts of radioactive material in soil and building structures, accessed November 11, 2016, at http://web.ead.anl.gov/resrad/datacoll/porosity.htm.

Bolin, B., 1958, On the use of tritium as a tracer for water in nature: Proceedings of the Second United Nations International Conference on the Peaceful Uses of Atomic Energy, Geneva, Switzerland, September 1–13, 1958, p. 336–344.

Bradley, D. Nathan, 2012, Slope-area computation program graphical user interface 1.0—A preprocessing and postprocessing tool for estimating peak flood discharge using the slope-area method: U.S. Geological Survey Fact Sheet 2012–3112, 4 p.

Burton, Bethany L., Powers, Michael H., and Ball, Lyndsay B., 2014, Characterization of subsurface stratigraphy along the lower American River floodplain using electrical resistivity, Sacramento, California, 2011: U.S. Geological Survey Open-File Report 2014–1242, 62 p.

Chapelle, Francis H., and Knobel, LeRoy L., 1985, Stable carbon isotopes of HCO_3 in the Aquia aquifer, Maryland—Evidence for an isotopically heavy source of CO_2: Ground Water, v. 23, no. 5, p. 592–599.

Chestnut, Peter C., 2012, Aamodt adjudication: Water Matters!, p. 8., accessed March 24, 2014, at http://uttoncenter.unm.edu/pdfs/Water-Matters-2013/Aamodt%20Adjudication%20.pdf.

Clark, Ian D., and Fritz, Peter, 1997, Environmental isotopes in hydrogeology: Boca Raton, Fla., CRC Press/Lewis Publishers, 328 p.

Craig, Harmon, 1961, Isotopic variations in meteoric waters: Science, v. 133, no. 3465, p. 1702.

Dalrymple, Tate, and Benson, M.A., 1967, Measurement of peak discharge by the slope-area method: U.S. Geological Survey Techniques of Water-Resources Investigations, book 3, chap. A2, 12 p. [Also available at http://pubs.usgs.gov/twri/twri3-a2/.]

Dam, William L., 1995, Geochemistry of ground water in the Gallup, Dakota, and Morrison aquifers, San Juan Basin, New Mexico: U.S. Geological Survey Water-Resources Investigations Report 94–4253, p. 76.

Dethier, David P., and Reneau, Steven L., 1995, Quaternary history of the western Española Basin, New Mexico, *in* Bauer, P.W., Kues, B.S., Dunbar, N.W., Karlstrom, K.E., and Harrison, B., eds., Geology of the Sante Fe Region: New Mexico Geological Society, 46th Annual Fall Field Conference Guidebook, p. 289–298.

Dillon, Peter, 2005, Future management of aquifer recharge: Hydrogeology Journal, v . 13, no. 313, p. 313–316.

Eberl, D.D., 2003, User's guide to RockJock—A program for determining quantitative mineralogy from powder X-ray diffraction data: U.S. Geological Survey Open-File Report 2003–78, 47 p.

Fishman, Marvin J., ed., 1993, Methods of analysis by the U.S. Geological Survey National Water Quality Laboratory—Determination of inorganic and organic constituents in water and fluvial sediments: U.S. Geological Survey Open-File Report 93–125, 217 p.

Fishman, Marvin J., and Friedman, Linda C., 1989, Methods for determination of inorganic substances in water and fluvial sediments: U.S. Geological Survey Techniques of Water-Resources Investigations, book 5, chap. A1, 545 p.

Friedman, Irving, Smith, George I., Gleason, Jim D., Warden, Augusta, and Harris, Joyce M., 1992, Stable isotope composition of waters in southeastern California—Modern precipitation: Journal of Geophysical Research, v. 97, no. d5, p. 5795–5812.

Galusha, Ted, and Blick, John C., 1971, Stratigraphy of the Santa Fe Group, New Mexico: Bulletin of the American Museum of Natural History, v. 144, article 1, New York, 127 p.

Garbarino, John R., 1999, Methods of analysis by the U.S. Geological Survey National Water Quality Laboratory—Determination of dissolved arsenic, boron, lithium, selenium, strontium, thallium, and vanadium using inductively coupled plasma-mass spectrometry: U.S. Geological Survey Open-File Report 99–093, 31 p.

Garbarino, John R., Kanagy, Leslie K., and Cree, Mark E., 2006, Determination of elements in natural-water, biota, sediment, and soil samples using collision/reaction cell inductively coupled plasma-mass spectrometry: U.S. Geological Survey Techniques and Methods, book 5, sec. B, chap. 1, 88 p.

Genereux, David P., and Hooper, Rick P., 1998, Oxygen and hydrogen isotopes in rainfall-runoff studies, *in* Kendall, C., and McDonnell, J.J., eds., Isotope tracers in catchement hydrology: Amsterdam, Elseveier Science B.V., p. 319–346.

Geophex, Ltd., 2015, GEM-2 broadband EMI sensor: Geophex Web page, accessed March 9, 2015, at http://www.geophex.com/Product%20-%20Hand-held%20Gem2.htm.

Hearne, Glenn A., 1985, Mathematical model of the Tesuque aquifer system near Pojoaque, New Mexico: U.S. Geological Survey Water-Supply Paper 2205, p. 75.

Hem, John D., 1985, Study and interpretation of the chemical characteristics of natural waters, 3rd edition: U.S. Geological Survey Water-Supply Paper 2254, 263 p.

HKM Engineering, 2008, Pojoaque regional water system engineering report, prepared for Northern Pueblo Tributary Water Rights Association: HKM Engineering, 68 p., accessed on March 24, 2014, at http://www.santafecountynm.gov/userfiles/AAEngRpt10b.pdf.

Ingraham, Neil L., 1998, Isotopic variations in precipitation, *in* Kendall, C., and McDonnell, J.J., eds., Isotope tracers in catchement hydrology: Amsterdam, Elsevier Science B.V., p. 87–118.

IRIS Instruments, 2015, Principles of geophysical methods for groundwater investigations: IRIS Instruments Web page, accessed January 20, 2015, at http://www.iris-instruments.com.

Johnson, A.I., 1963, A field method of measurement of infiltration: U.S. Geological Survey Water-Supply Paper 1544-F.

Johnson, P.S., Koning, D.J., and Partey, F.K., 2013, Shallow groundwater geochemistry in the Española Basin, Rio Grande rift, New Mexico—Evidence for structural control of a deep thermal source, *in* Hudson, M.R., and Grauch, V.J.S., eds., New perspectives on Rio Grande rift basins—From tectonics to groundwater: Geological Society of America Special Paper 494, p. 261–301.

Jury, William A., Gardner, Wilford R., and Gardner, Walter H., 1991, Soil physics (5th ed.): Hoboken, N.J., John Wiley & Sons, Inc., 552 p.

Kelley, Vincent C., 1978, Geology of the Española Basin, New Mexico: New Mexico Bureau of Mines and Mineral Resources Geologic Map 48, scale 1:125,000.

Kelley, Vincent C., 1979, Geomorphology of the Española Basin, New Mexico, *in* Ingersoll, R.V., Woodward, L.A., and James, H.L., eds., New Mexico Geological Society 30th Annual Fall Field Conference Guidebook: New Mexico Geological Society, p. 281–288.

Kendall, Carol, and Coplen, Tyler B., 2001, Distribution of oxygen-18 and deuterium in river waters across the United States: Hydrological Processes, v. 15, no. 7, p. 1363.

Koning, Daniel J., and Read, Adam S., 2010, Geologic map of the southern Española Basin, Santa Fe County, New Mexico: New Mexico Bureau of Mines and Mineral Resources, Open-File Report 531, 36 p., 2 pls.

Longmire, Patrick, Dale, Michael, Counce, Dale, Manning, Andrew, Larson, Toti, Granzow, Kim, Gray, Robert, and Newman, Brent, 2007, Radiogenic and stable isotope and hydrogeochemical investigation of groundwater, Pajarito Plateau and surrounding areas, New Mexico: Los Alamos, N. Mex., Los Alamos National Laboratory, Report LA-14333.

Lucas, L.L., and Unterweger, M.P., 2000, Comprehensive review and critical evaluation of the half-life of tritium: Journal of Research of the National Institute of Standards and Technology, v. 105, no. 4, p. 541–549.

Lucius, Jeffrey E., Langer, William H., and Ellefsen, Karl J., 2007, An introduction to using surface geophysics to characterize sand and gravel deposits: U.S. Geological Survey Circular 1310, 33 p.

Manning, Andrew H., 2008, Groundwater temperature, noble gas and carbon isotope data from the Española Basin, New Mexico: U.S. Geological Survey Scientific Investigations Report 2008–5200, 69 p.

Manning, Bruce A., and Goldberg, Sabine, 1997, Adsorption and stability of arsenic (III) at the clay mineral-water interface: Environmental Science and Technology, v. 31, p. 2005–2011.

McAda, Douglas P., and Wasiolek, Maryann, 1988, Simulation of the regional geohydrology of the Tesuque aquifer system near Santa Fe, New Mexico: U.S. Geological Survey Water Resources Investigation Report 87–4056, 71 p.

McLemore, Virginia T., Vaniman, David, McQuillan, Dennis, and Longmire, Patrick, 2011, Uranium deposits in the Española Basin, Santa Fe County, New Mexico, *in* Koning, D.J., Karlstrom, K.E., Kelley, S.A., Lueth, V.W., and Aby, S.B., eds., New Mexico Geological Society guidebook, 62nd field conference, geology of the Tusas Mountains–Ojo Caliente, p. 399–408.

McQuillan, Dennis, and Montes, Ray, 1998, Groundwater geochemistry, Pojoaque Pueblo, New Mexico: New Mexico Environment Department, Groundwater Quality Bureau, in cooperation with the Pueblo of Pojoaque Environment Department, 34 p.

Mook, Willem G., and van der Plicht, Johannes, 1999, Reporting ^{14}C activities and concentrations: Radiocarbon, v. 41, p. 227–239.

Multiphase Technologies, 2015, 3D Electrical Resistivity Tomography Inversion Software: Multiphase Technologies Web page, accessed March 9, 2015, at http://mpt3d/software.html.

Murphy, Ellyn M., Ginn, Timothy R., and Phillips, Jerry L., 1996, Geochemical estimates of paleorecharge in the Pasco Basin; evaluation of the chloride mass balance technique: Water Resources Research, v. 32, no. 9, p. 2853.

National Geodetic Survey, 2015, OPUS: Online Positioning User Service, accessed October 8, 2015, at http://www.ngs.noaa.gov/OPUS/.

National Ocean Sciences Accelerator Mass Spectrometry Facility, 2015, General statement of ^{14}C procedures at the National Ocean Sciences AMS Facility: National Ocean Sciences Accelerator Mass Spectrometry Web page, accessed July 2015 at http://www.whoi.edu/nosams/general-statement-of-14c-procedures.

National Research Council, 2008, Prospects for managed underground storage of recoverable water: National Academy Press, 350 p.

New Mexico Environment Department, 2015, Risk assessment guidance for site investigation and remediation: New Mexico Environment Department, v. 1, 276 p.

Phillips, Fred, 1994, Environmental tracers for water movement in desert soils of the American Southwest: Soil Science Society of America journal, v. 58, no. 1, p. 15.

Phillips, Fred M., Peeters, Leslie A., and Tansey, Michael K., 1986, Paleoclimatic inferences from an isotopic investigation of groundwater in the central San Juan Basin, New Mexico: Quaternary Research, v. 26, no. 2, p. 179–193.

Plummer, L. Niel, Bexfield, Laura M., Anderholm, Scott K., Sanford, Ward E., and Busenberg, Eurybiades, 2012, Geochemical characterization of ground-water flow in the Santa Fe Group aquifer system, Middle Rio Grande Basin, New Mexico (ver. 1.2, November 20, 2012): U.S. Geological Survey Water-Resources Investigations Report 03–4131, 395 p., CD-ROM in pocket. [Also available at http://pubs.usgs.gov/wri/wri034131/.]

Plummer, L. Niel, and Friedman, Linda C., 1999, Tracing and dating young ground water: U.S. Geological Survey Fact Sheet 134–99, p. 4.

Plummer, L. Niel, and Glynn, Pierre D., 2013, Radiocarbon dating in groundwater systems, *in* International Atomic Energy Agency, ed., Isotope methods in dating old groundwater: Vienna, Austria, International Atomic Energy Agency, p. 33–89.

Révész, Kinga, and Coplen, Tyler B., 2008a, Determination of the $\delta(^{2}H/^{1}H)$ of water—RSIL lab code 1574, *in* Révész, K., and Coplen, T.B., eds., Methods of the Reston Stable Isotope Laboratory: U.S. Geological Survey Techniques and Methods, book 10, chap. C1, 27 p.

Révész, Kinga, and Coplen, Tyler B., 2008b, Determination of the $\delta(^{18}O/^{16}O)$ of water—RSIL lab code 489, *in* Révész, K., and Coplen, T.B., eds., Methods of the Reston Stable Isotope Laboratory: U.S. Geological Survey Techniques and Methods, book 10, chap. C2, 28 p.

Robertson, Andrew J., Ranalli, Anthony J., Austin, Stephen A., and Lawlis, Bryan R., 2016, The source of groundwater and solutes to Many Devils Wash at a former uranium mill site in Shiprock, New Mexico: U.S. Geological Survey Scientific Investigations Report 2016–5031, 54 p., http://dx.doi.org/10.3133/sir20165031.

Spiegel, Zane, and Baldwin, Brewster, 1963, Geology and water resources of the Santa Fe area: New Mexico Geological Survey Water-Supply Paper 1525, 258 p.

Stumm, Werner, and Morgan, James J., 1996, Aquatic chemistry (3rd ed.): New York, John Wiley and Sons, 1022 p.

Thomas, C.L., Stewart, A.E., and Constantz, Jim, 2000, Determination of infiltration and percolation rates along a reach of the Santa Fe River near La Bajada, New Mexico: U.S. Geological Survey Water-Resouces Investigations Report 00–141, 65 p.

Turf-Tec International, 2014, Large volume Mariotte tubes for use with 12 and 24 inch diameters infiltration rings: Turf-Tec International Web page, accessed November 10, 2014, at http://www.turf-tec.com/IN13Lit.html.

U.S. Army Corps of Engineers, 2010, HEC-RAS river analysis system, user's manual, version 4.1: U.S. Army Corps of Engineers Hydrologic Engineering Center, 790 p.

U.S. Environmental Protection Agency, 2009, National Primary Drinking Water Regulations: U.S. Environmental Protection Agency EPA 816-F-09-004, 6 p.

U.S. Environmental Protection Agency, variously dated, Test methods for evaluating solid waste, physical / chemical methods (3d ed.): U.S. Environmental Protection Agency SW-846.

U.S. Geological Survey, variously dated, National field manual for the collection of water-quality data: U.S. Geological Survey Techniques of Water-Resources Investigations, book 9, chaps. A1–A9. [Also available at http://water.usgs.gov/owq/FieldManual/.]

University of Miami Tritium Laboratory, 2016, Tritium procedures and standards: University of Miami Web page, accessed July 2016 at http://www.rsmas.miami.edu/groups/tritium/analytical-services/procedures-and-standards/tritium/.

Wang, Yang, Huntington, Thomas G., Osher, Laurie J., Wassenaar, Leonard I., Trumbore, Susan E., Amundson, Ronald G., Harden, Jennifer W., McKnight, Diane M., Schiff, Sherry L., Aiken, George R., Lyons, W. Berry, Aravena, Ramon O., and Baron, Jill S., 1998, Carbon cycling in terrestrial environments, *in* Kendall, Carol, and McDonnell, J.J., eds., Isotope tracers in catchment hydrology: Elsevier Science B.V., Amsterdam, p. 577–610.

Western Regional Climate Center, 2016, Period of record monthly climate summary for Española, NM: Western Regional Climate Center Web page, accessed January 18, 2016, at http://www.wrcc.dri.edu/cgi-bin/cliMAIN.pl?nm3031.

Wigley, T.M.L., Plummer, L.N., and Pearson, F.J., 1978, Mass transfer and carbon isotope evolution in natural water systems: Geochimica et Cosmochimica Acta, v. 42, no. 8, p. 1117–1139.

Wood, Warren W., 1999, Use and misuse of the chloride-mass balance method in estimating ground water recharge: Ground Water, v. 37, no. 1, p. 2.

Yune, Tae-Won, T., Choi, Chan-Ho, and Im, Gi-Hong, 2006, Single carrier frequency-domain equalization with transmit diversity over mobile multipath channels: IEICE Transactions on Communications, v E89-B, no. 7, p. 2050–2060.

Zohdy, A.A., Eaton, G.P., and Mabey, D.R., 1974, Application of surface geophysics to ground-water investigations: U.S. Geological Survey Techniques of Water-Resources Investigations, book 2, chap. D1, 116 p.

Publishing support provided by
Lafayette Publishing Service Center

ISSN 2328-0328 (online)
https://doi.org/10.3133/sir20175007